

Efforts Toward the Design and Synthesis of a Synthetic  
Platform Toward Novel Aminoglycoside Antibiotics

By

Nainoa Norman Ing

Thesis

Submitted to the Faculty of the  
Graduate School of Vanderbilt University  
in partial fulfillment of the requirements

for the degree of

MASTER OF SCIENCE

In Chemistry

May 10, 2024

Nashville, Tennessee

Approved:

Steven D. Townsend, Ph.D.

Jennifer A. Gaddy, Ph.D.

This work is dedicated to all the people who have supported me through my journey.

## ACKNOWLEDGMENTS

If I have sailed far, it could only be because there were people with me weathering the storm, repairing the ship, and helping me chart my course. I will never forget these shores, smiles, and struggles we have shared. As I navigate the turbulent waters ahead, I ask that you continue to watch over me and my work. I hope I can make you proud and leave a legacy that honors all the time and energy you have invested in me. Know that I will take these experiences and lessons with me and use them on my journey, regardless of where the wind may blow me.

I also want to specifically thank Dr. Steve Townsend for his continued time and energy on my behalf. The patience and benevolence which I experienced while learning from you will forever be examples I strive to emulate.

To my parents, thank you for supporting me and raising me right. Thank you for giving me tough love and challenging me to be better each and every day. Your support and tough love kept me from reaching the darkest points of despair.

To my partner, Andrea, thank you for sticking with me through this whole rollercoaster of life. When I was struggling you were a guiding light that helped me chart my course through a dark and stormy sea.

Finally, here's the obligatory thank you for the funding. I am grateful that I was given a chance to improve myself and learn about the laws of this world.

Research reported in this publication was supported by the National Institute of General Medical Sciences of the National Institutes of Health under Award Number R35GM133602. The content is solely the responsibility of the author and does not necessarily represent the official views of the National Institutes of Health.

# TABLE OF CONTENTS

Page

<b>LIST OF TABLES.....</b>	<b>v</b>
<b>LIST OF FIGURES.....</b>	<b>vi</b>
<b>1 Chapter 1: Antibiotics and Resistance .....</b>	<b>1</b>
1.1 Introduction.....	1
1.2 Historical Context .....	1
1.3 Resistance.....	2
1.3.1 Resistance: Prevention .....	3
1.3.2 Resistance: Drug Modification .....	4
1.3.3 Resistance: Target Modification .....	5
1.4 Conclusion .....	6
<b>2 Chapter 2: Aminoglycoside Antibiotics .....</b>	<b>7</b>
2.1 Introduction.....	7
2.2 AGA Structure.....	8
2.3 AGA Uptake .....	9
2.4 AGA Activity.....	10
2.5 AGA Resistance.....	11
2.5.1 AGA Resistance: Prevention .....	11
2.5.2 AGA Resistance: Drug Modification .....	11
2.5.3 AGA Resistance: Target Modification .....	12
2.6 Combatting Resistance .....	13
<b>3 Chapter 3: Scaffold Design and Progress.....</b>	<b>14</b>
3.1 Introduction.....	14
3.2 AGA Design Platform .....	15
3.3 Synthetic Strategy.....	16
3.4 Synthesis of (3.4) .....	17
3.5 Synthesis of (3.2) .....	18
3.6 Synthesis of (3.3) .....	19
3.7 Synthesis of (3.5) .....	20
3.8 Glycosylation Strategy and Final Maneuvers .....	21
3.9 Conclusion .....	22
General Methods.....	23
Instrumentation.....	23
Synthetic Procedures.....	24
<b>References: .....</b>	<b>31</b>

## LIST OF TABLES

Table	Page
2.1 Discovery of Representative AGAs.....	7

## LIST OF FIGURES

Figure	Page
1.1 Early Antibiotics .....	1
1.2 Gram-negative cell antibiotic uptake and methods of resistance .....	3
1.3 Bacterial resistance from enzymatic drug modification .....	4
1.4 Bacterial Resistance from drug target modification .....	5
2.1 AGA core structures and parent compounds .....	8
2.2 <i>E. coli</i> A-site closed to open form and neomycin hydrogen bonding activity within A-site .....	10
2.3 Latest generation AGA plazomicin and parent sisomicin, structural improvements in red.....	13
3.1 Challenges to parent neomycin scaffold and novel AGA (3.1) with improvements .....	15
3.2 Novel AGA (3.1) and retrosynthetic analysis to building blocks (3.2), (3.3), (3.4), and (3.5) ..	16
3.3 Synthesis of 2-deoxyribose building block .....	17
3.4 Synthetic progress toward <i>gem</i> -difluoromethylene building block .....	18
3.5 Synthetic route to 2-DOS building block .....	19
3.6 Synthetic route to building block from (S,S)-pseudoephedrine glycinamide.....	20
3.7 Glycosylation strategy and late stage manipulations toward novel AGA.....	21

# Chapter 1 Antibiotics and Resistance

## 1.1 Introduction

“My dear, here we must run as fast as we can, just to stay in place. And if you wish to go anywhere you must run twice as fast as that.” -Lewis Carroll, *Through the Looking-Glass*

In 1973 Leigh Van Valen proposed the red queen hypothesis to explain the observations we had made between species.<sup>1</sup> Species must “run” or evolve just to survive. If a rabbit evolves faster legs to escape, a fox that hunts this rabbit for sustenance is forced to evolve and overcome this new trait. This prompts the cycle to repeat as species “run” as fast as they can just to stay in place. Since our first predecessors, humans have been locked in this evolutionary race with our greatest adversary, bacteria. Our bodies evolve to purge bacterial invaders, and the bacterial invaders evolve to overcome our adaptations. That is, until the critical discovery of antibiotics.

## 1.2 Historical Context

Antibiotics, molecules with the ability to kill or at the very least inhibit the growth of bacteria and other micro-organisms, are arguably one of mankind’s most crucial discoveries. This scientific advancement allows us to combat microorganisms without having to undergo the painful, and lengthy process of natural selection. These critical tools began with the seminal work of Paul Ehrlich in the late 1800s.<sup>2,3</sup> Ehrlich had envisioned a “magic bullet” which while deadly to a pathogen, could be survived by the host. After 605 compounds, Ehrlich came across compound 606, Arsphenamine, which would become commonly known as Salvarsan (**1.1**), the first cure for syphilis<sup>4,5</sup>. In a world which had thought that these diseases were inescapable curses, Ehrlich had proven that we could fight back.

Ehrlich’s success led the German conglomerate, IG Farben to begin investigating synthetic cures with the hypothesis that dyeing activity was directly related to drug action.<sup>3,6,7</sup> Their extensive screening led them to the dye KL730, sulfamidochrysoidine, eventually known as Prontosil (**1.2**).

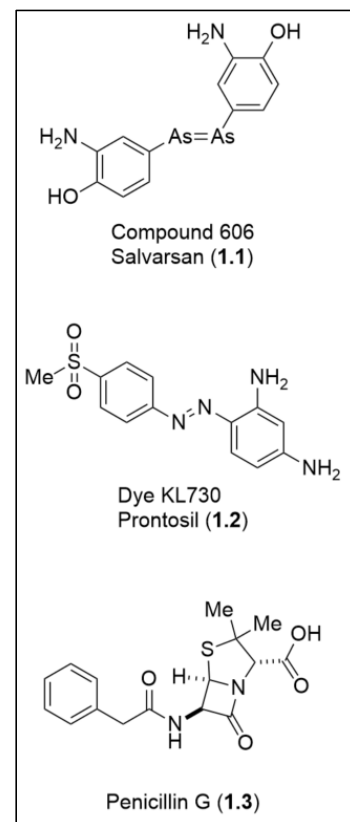


**Figure 1.1** Early Antibiotics

Prontosil became the first in class of the sulfa-drugs, cures for streptococcal infections. While these discoveries were major strides toward modern medicinal chemistry, the start of the antibiotic era would only begin after Alexander Flemings's serendipitous discovery of penicillin (**1.3**) from mold that had grown amidst colonies of plated *Staphylococcus* bacteria.<sup>6, 8</sup>

The discovery of penicillin was the paradigm shift which gave us the power to treat a broad swath of infections such as pneumonia, gonorrhea, and rheumatic fever. Before this wonder drug, a simple scratch and resultant infection could have proved deadly. Importantly, the discovery of penicillin, an antibiotic isolated from the fungus *Penicillium rubrum*, guided our approach to antibiotics toward natural products.<sup>5, 9</sup> Natural products are tool compounds created by other organisms as evolutionary adaptations. Discovering and copying the tools of nature, we entered the golden age of antibiotics (1945-1960s) which saw the discovery of much of the arsenal we employ today.

### 1.3 Resistance

Since our discovery of the miracle of antibiotics, widespread misuse and overuse has led to the emergence of antibiotic resistant bacteria. Furthermore, the rate at which novel antibiotics have been discovered has seen a sharp decline in recent years.<sup>5, 10</sup> Coupled with the economic pressures and timelines of drug development, it is unsurprising that many large pharmaceutical companies fear a lack of return when developing new antibiotics and have exited the space.<sup>3, 10</sup> Today, multidrug resistant bacteria and a lack of new treatments present a serious, growing threat to humanity.<sup>5, 11</sup>

To combat the evolution and emergence of drug-resistant bacteria, one must first understand how antibiotic resistance is caused and what forms it manifests as. Antibiotic resistance is the evolutionary adaptation of an organism to the selective pressure of antibiotics.<sup>10</sup> Within each population of bacteria, there exists the chance that one or multiple members contain adaptations which help them survive antibiotic treatment. These adaptations are carried forward to the next generation and can even be refined over time.<sup>10</sup> To complicate these matters further, horizontal gene transfer can confer bacterial resistance not just to progeny, but to other bacteria via mobile genetic elements.<sup>10, 13</sup> This means that antibiotic usage comes with the risk of selecting for and developing bacterial species which render our current antibiotic arsenal obsolete.



### 1.3.1 Resistance: Prevention

Bacterial resistance manifests in three general categories: drug modification, target modification, and prevention strategies.<sup>10, 14</sup> Resistance begins with prevention of cellular uptake and retention within the intracellular space where many drug targets lie. Prevention strategies (**Figure 1.2**) focus on barriers to cellular entry and actively pumping antibiotics out of the cell through efflux pumps. Gram-negative bacteria possess both an internal and external membrane which serves as a critical defense preventing many antibiotics and toxic compounds from penetrating the cell.<sup>15</sup> The tightly packed lipopolysaccharides (LPS) of the outer membrane limit hydrophobic compound entry through diffusion across this lipid bilayer.<sup>15, 16</sup> The porins of the outer membrane limit hydrophilic species through downregulation or modification of existing channels.<sup>16, 17</sup> If antibiotics manage to make it past the barriers, these bacteria can use efflux pumps to expel the toxic substance before lethal concentrations are reached.<sup>13, 18-21</sup> These efflux pumps can confer resistance to a wide range of antibiotics.<sup>21</sup>

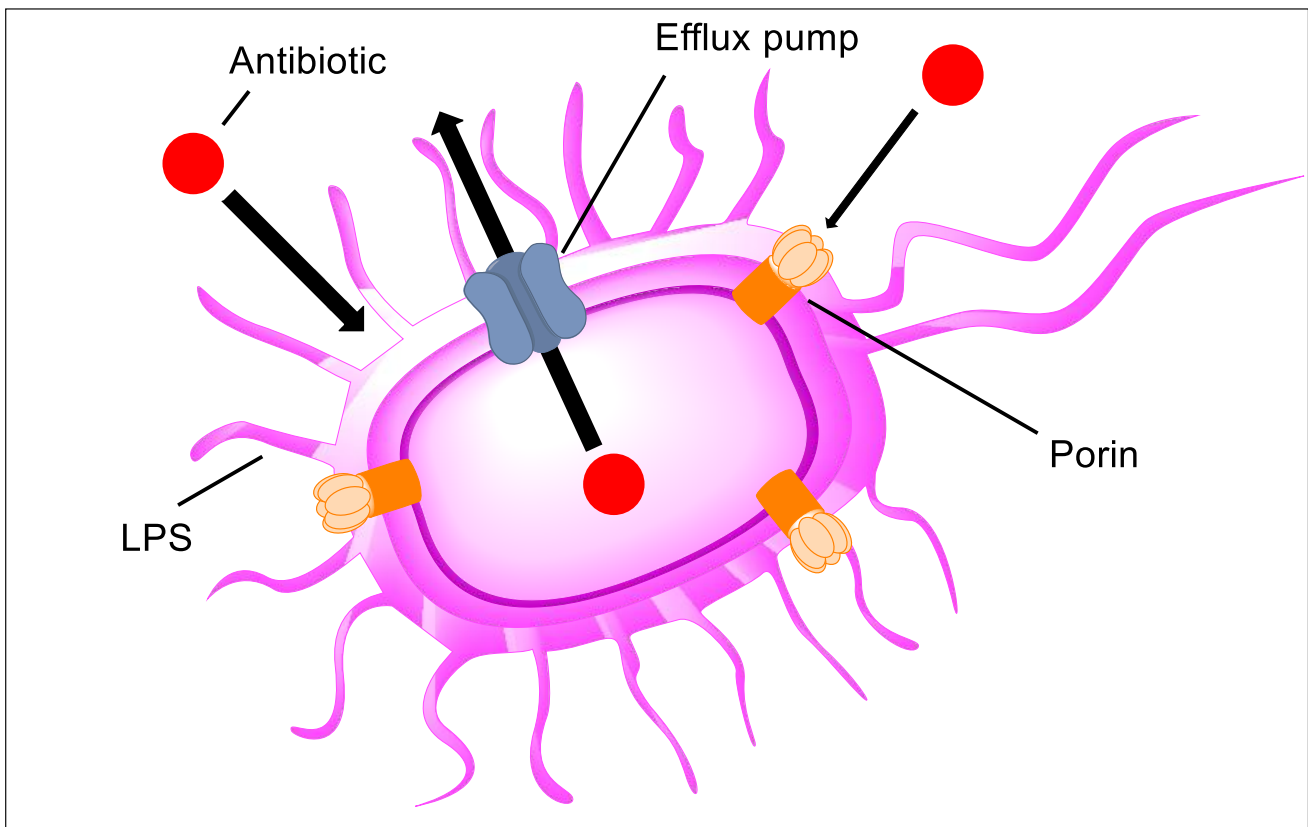


**Figure 1.2** Gram-negative cell antibiotic uptake and methods of resistance

### 1.3.2 Resistance: Drug Modification

Once a drug has made it inside of the cell, resistance takes the form of enzymes. Drug modification strategies (**Figure 1.3**) utilize target-specific enzymatic modifications to erode drug affinity and efficacy. These enzymatic modifications can target and destroy key functional sites of the drug such as the hydrolysis of the  $\beta$ -lactam of penicillin by  $\beta$ -lactamases.<sup>22</sup> In other cases, they can work to attach different functional groups such as acetyl, phosphoryl, thio, nucleotidyl, or glycosyl groups thereby altering the sterics or electronics of the drug seen in the aminoglycosides case.<sup>23-25</sup> These modifications serve to prevent key interactions such as hydrogen bonding to target sites.

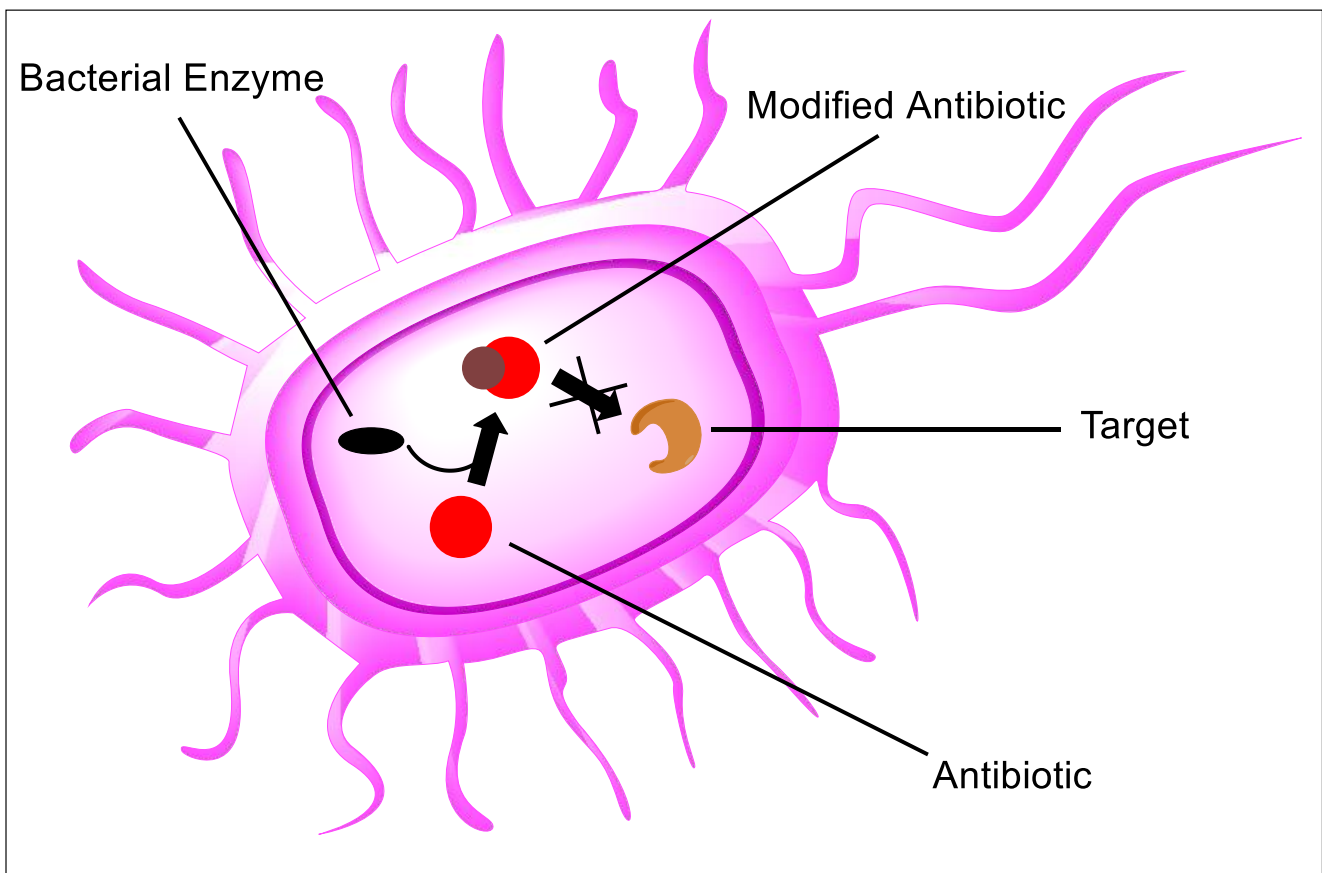


**Figure 1.3** Bacterial resistance from enzymatic drug modification

### 1.3.3 Resistance: Target Modification

The last and most common layer of defense for the bacteria manifests as modification of the drug target (**Figure 1.4**).<sup>14</sup> This strategy allows the bacteria to add modifications which reduce drug target affinity or activity. This can arise from a point mutation of the target encoding genes, enzymatic modification, decoys, or bypass of the target.<sup>14</sup> Methylation of target site by ribosomal methyltransferases is a common form of resistance found in ribosome-targeting antibiotics such as aminoglycosides, macrolides, and oxazolidinones.<sup>14</sup> This methyl group serves to add a steric hinderance to lower target affinity. The use of decoys can be seen in quinolone antibiotic resistance. Quinolone resistance protein is expressed and acts as a DNA mimic which engages in competitive binding with Topo II, DNA gyrase, and Topo IV enzymes.<sup>14, 26</sup> This activity decreases the window of formation of the lethal DNA-quinolone complexes.<sup>26</sup>

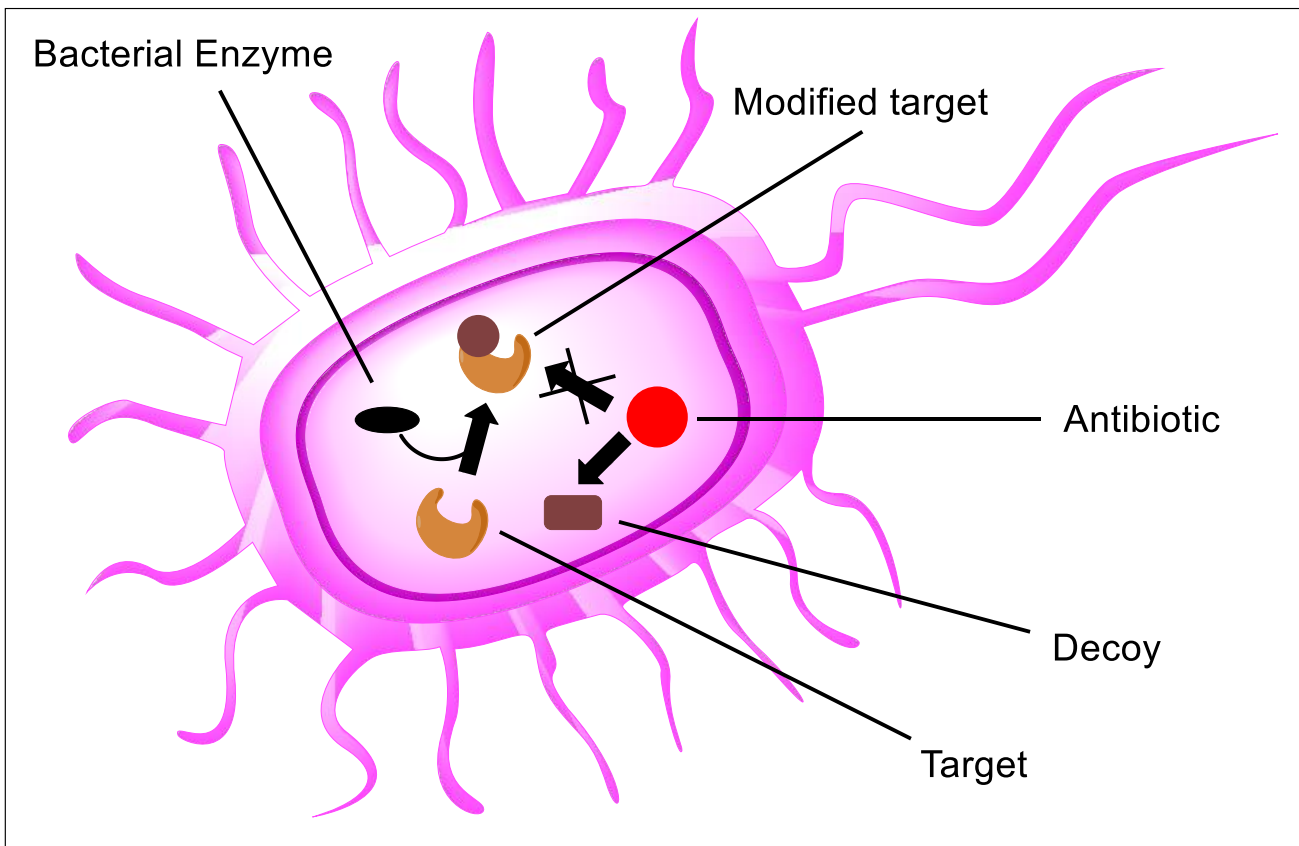


**Figure 1.4** Bacterial resistance from drug target modification

## *1.4 Conclusion*

Today, multidrug-resistant bacteria are a serious, growing problem. Importantly, multidrug-resistant Gram-negative pathogen have evolved resistance to all known major antibiotic classes and present a critical threat.<sup>5, 12, 27</sup> The discovery and introduction of antibiotics gave us tools that other organisms had developed to fight these bacteria; however, it has also led to bacterial evolution. A new, evolutionary approach is needed if we are to continue having useful antibiotics. Borrowing from Lewis Carroll again, we are once again locked in an arms race where “we must run as fast as we can, just to stay in place. And if you wish to go anywhere you must run twice as fast as that.”

## Chapter 2: Aminoglycoside Antibiotics

### 2.1 Introduction

Aminoglycoside antibiotics (AGAs) are potent, broad-spectrum, high efficacy weapons against both Gram-positive and Gram-negative bacteria. Streptomycin, the first in class AGA, was discovered and isolated from the soil-dwelling bacteria *Streptomyces griseus* by Selman Waksman in 1943.<sup>28</sup> AGAs target the bacterial ribosome to disrupt the critical process of protein synthesis which leads to their antibiotic activity. Introduced into the clinic in the mid-1940s, it would become the first antibiotic to successfully treat tuberculosis and continues to be used to this day. The success of streptomycin led to the discovery and introduction of new AGAs including neomycin (1949), gentamycin (1963), tobramycin (1967), and sisomicin (1970).<sup>29</sup> While AGAs are still clinically relevant today, the introduction of new antibiotics containing fewer side effects such as carbapenems and fluoroquinolones in the 1970s and 1980s diminished interest and development of AGAs. Bacterial resistance and immunity, particularly in Gram-negative species, has renewed interest in these potent bactericidal compounds with the most recent addition of plazomicin, a semisynthetic AGA from sisomicin developed by Achaogen.<sup>30</sup>

**Table 2.1: Discovery of Representative AGAs**

Entry	AGA	Source	Year
1	Streptomycin	<i>Streptomyces griseus</i>	1944
2	Neomycin	<i>Streptomyces fradiae</i>	1949
3	Paromomycin	<i>Streptomyces rimosus forma paromomycinus</i>	1956
4	Kanamycin	<i>Streptomyces kanamyceticus</i>	1957
5	Gentamicin	<i>Micromonospora purpurea</i>	1963
6	Tobramycin	<i>Streptomyces tenebrarius</i>	1967
7	Apramycin	<i>Streptomyces tenebraius</i>	1968
8	Sisomicin	<i>Genus micromonospora</i>	1970
9	Butirosin	<i>Bacillus circulans</i>	1971

## 2.2 AGA Structure

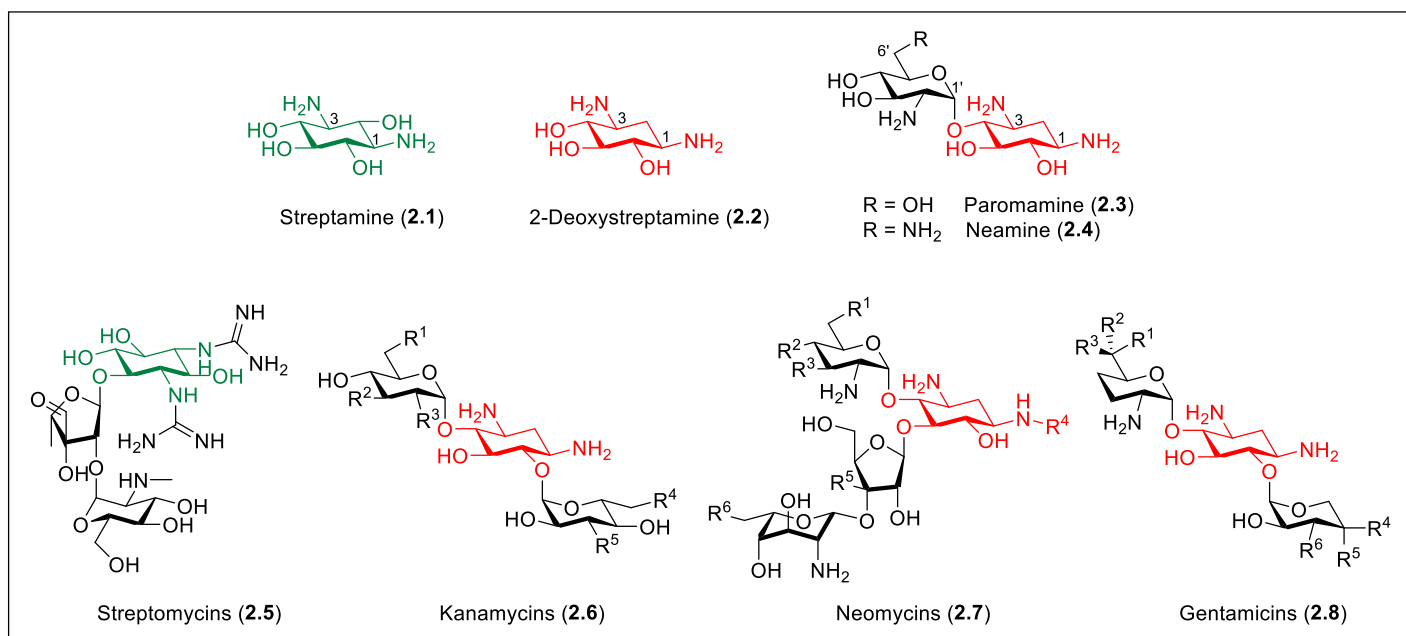


**Figure 2.1** AGA core structures and parent compounds

The term ‘aminoglycoside’ broadly refers to a carbohydrate bearing an amino functionality. The AGA structure consists of one or several of these aminosugars connected by pseudo-glycosidic linkages to a diaminocyclitol ring. Many AGAs contain a common paromamine core with the 2-deoxystreptamine (2-DOS) (**Figure 2.1**) (2.2) substructure being appended at the 5- and 6- positions leading to the 4,5- or 4,6-AGA classifications. The predominant chemical species of the 4,5-AGAs are the neomycin, paromomycin, and ribostamycin families whereas the 4,6-AGAs contain the gentamicin, kanamycin, and netilmicin families. While a myriad of AGAs exist, apart from spectinomycin, AGAs not derived from paromamine have borne little to no clinical significance.<sup>29</sup> Of the paromamine-derived AGAs, the three major classes are the kanamycins (2.6), neomycins (2.7), and gentamicins (2.8). Kanamycins contain a 4,6-disubstituted 2-DOS linked to both a 3-aminoglucose and 2,6-diaminoglucose. Neomycins contain a 4,5-disubstituted 2-DOS linked to both a furanose and one or two aminoheptose units. Lastly, gentamicins contain a 4,6-disubstituted 2-DOS linked to both a furanose and one or two aminoheptose units which can contain additional carbon side chains.<sup>29</sup> Notably, all 2-DOS based AGAs in clinical use are 4,6-AGAs.<sup>31</sup>

### *2.3 AGA Uptake*

To engage in their antibiotic activity, AGAs must first enter the cell. Cellular uptake of AGAs is hypothesized to first begin with electrostatic interaction between positively charged AGAs and the negatively charged LPS of the bacterial outer membrane.<sup>32, 33</sup> The amino groups of the AGAs are heavily protonated under physiological conditions and this strongly cationic nature is thought to drive this nonspecific interaction. The cell then enters an energy dependent phase 1 (EDP1) which is characterized by slow uptake correlated to AGA concentration. In this step, the aminoglycoside must move through the periplasmic space and be transported through the inner membrane. Oxidative phosphorylation and electron transport are necessary since inhibitors of these processes block uptake.<sup>34</sup> Energy dependent phase 2 (EDP2) leads to a rapid accumulation of AGAs and uses energy from electron transport and adenosine triphosphate (ATP) hydrolysis. During this phase the AGAs bind to the bacterial 30S ribosomal subunit, interfering with protein synthesis.<sup>34</sup> The induced misreading during protein translation compromises cytoplasmic membrane integrity and function resulting in increased AGA uptake, further protein translation errors, and repetition of this cycle until cell death.<sup>35</sup>

## 2.4 AGA Activity

AGAs influence protein synthesis by direct interaction with ribosomal RNA, resulting in codon misreading or the inhibition of the tRNA-mRNA complex translocation.<sup>36</sup> The specific target is the open, decoding A-site (**Figure 2.2**) of the aminoacyl-tRNA acceptor site, located on helix 44 of the 16S rRNA subunit.<sup>37</sup> Generally, AGAs form high-affinity hydrogen bonding complexes with three unpaired adenine residues in the decoding loop, displacing the non-complementary adenines (A1492 and A1493) locking them into a “flipped-out” orientation.<sup>38</sup> This interaction serves to stabilize the decoding state with both A1492 and A1493 outside of the internal loop serving to allow noncognate tRNA to bind and be misread leading to the synthesis of faulty proteins.<sup>37</sup>

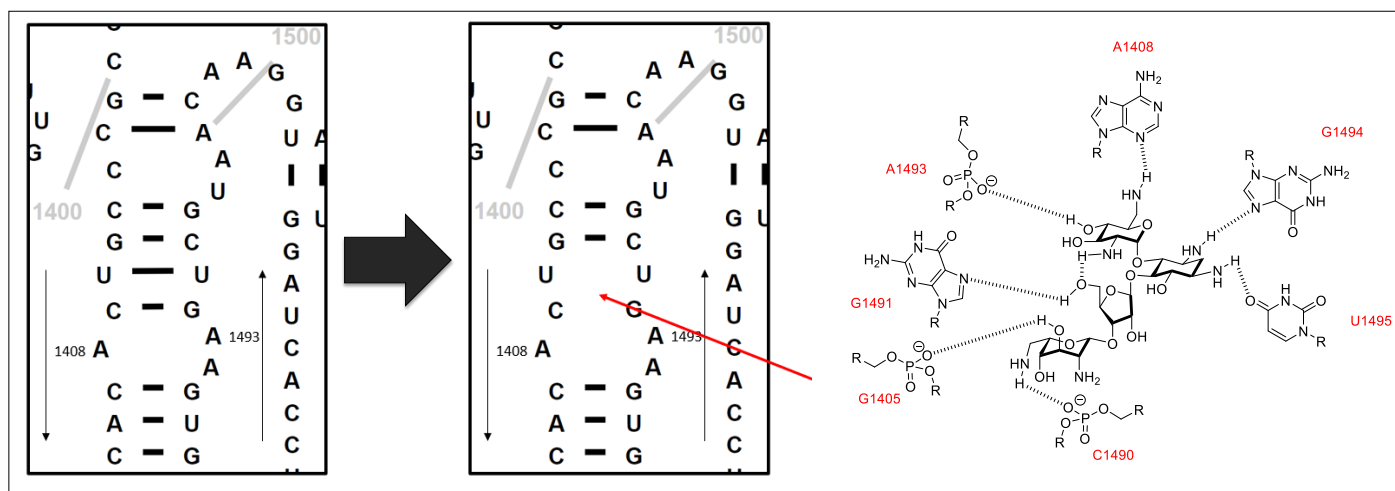


**Figure 2.2** *E. coli* A-site closed to open form (left) and neomycin hydrogen bonding activity within A-site RNACentral; 16S rRNA from *E. coli*, PDB3J9Z, chain SA; Generated by R2DT using EC\_SSU\_3D template by RiboVision (10.10.22)

The neamine/paromamine core serves as the main hydrogen bonding partner utilizing the 6'-substituent and ring oxygen to form stable complexes with the N1 and N6 of the highly conserved A1408 of the rRNA.<sup>39</sup> The 2-DOS subunit hydrogen bonds to U1406, U1495, and G1494. The upper glucosamine unit can bind A1407, A1493, A1492, and G1491 depending on substitution patterns.<sup>39</sup> Additional rings may impact specificity.



### *2.5.1 AGA Resistance: Prevention*

Widespread misuse and overuse of AGAs has resulted in a significant amount of bacterial resistance. These forms of resistance have manifested in all three of the previously discussed strategies in chapter one. The first layer of defense is barrier to cellular entry and intracellular concentration control via efflux pumps. Changes in the negative charge of the LPS of the outer membrane of bacteria have been shown to confer AGA-resistance.<sup>40-42</sup> This is likely due to weaker electrostatic interactions involved in initial drug-cell association during uptake. Due to the oxygen dependent nature of AGA entry to the cell discussed earlier, anaerobic bacteria are naturally resistant to AGAs.<sup>43</sup> Furthermore, any changes which lead to defective electron transfer chain components generate bacterial resistance if the bacteria can survive them.<sup>44-46</sup> Energy-dependent multidrug efflux pumps have been observed in resistant strains.<sup>47</sup>

### *2.5.2 AGA Resistance: Drug Modification*

The second strategy, drug modification, is the primary driver of antibiotic resistance in clinical bacterial isolates.<sup>48</sup> Three main types of aminoglycoside modifying enzymes (AMEs) have been identified and are discussed below.

Aminoglycoside acetyltransferases (AACs) are AMEs that have been identified in both Gram-positive and Gram-negative pathogen.<sup>49</sup> AACs catalyze the regioselective N-acetylation of the AGA by an acetyl-CoA donor. Of the nearly 50 known members of the AACs, AAC(1), AAC(3), AAC(2'), and AAC(6') are the main categories.<sup>29</sup> AAC(6') targets the 6'-amino group which plays a crucial role in AGA-rRNA binding and in doing so renders many useful AGA ineffective.<sup>38</sup>

Aminoglycoside phosphotransferases (APHs) are a group of AMEs mainly observed in Gram-positive bacteria. APHs are kinases which catalyze the regiospecific O-phosphorylation of the  $\gamma$ -phosphoryl group from an ATP donor to an alcohol of the AGA. The introduction of a phosphate group drastically affects the affinity of the AGA-rRNA interaction.<sup>50, 51</sup> The APHs can be classified into the APH(4)-I, APH(6)-I, APH(9)-I, APH(3')-I to -VII, APH(2'')-I to -IV, APH(3'')-I, and APH(7'')-I subcategories.<sup>29</sup> The largest of these, APH(3')s, is widely disseminated within the Gram-positive bacteria and has been used as a traceable resistance marker. APH(2'') is responsible for much of the resistance to the clinically used 4,6-AGAs, namely gentamicin.<sup>52</sup>

Aminoglycoside nucleotidyltransferases (ANTs) are a group of AMEs that are responsible for a significant amount of Gram-negative AGA resistance.<sup>53</sup> ANTs catalyze the O-adenylation of AGAs by Mg-ATP donors. The main groups of ANTs are ANT(6), ANT(9), ANT(4'), ANT(3''), and ANT(2'').<sup>29</sup> While a small group overall, adenylation by ANT(2'')s confer resistance to our clinically relevant 4,6-AGAs.<sup>53</sup>

### 2.5.3 Resistance: Target Modification

Lastly, bacteria can use the third defense strategy, drug target modification. Utilizing rRNA methyltransferases, these enzymes can methylate the 16S rRNA at the critical N(1) of A1408 or N(7) of G1405, positions crucial to drug binding.<sup>54</sup> Methylation of G1405 adds steric hinderance which prevents critical hydrogen bonding interactions for known 4,6-AGAs.<sup>55</sup> Methylation of A1408 prevents the 6'-amino group hydrogen bonding interaction and confers resistance to nearly all known AGAs.<sup>55</sup> Originally these methyltransferases were thought to be an evolutionary adaptation restricted to AGA producing bacteria to protect themselves from their own weapons and this form of resistance is not currently of clinical significance.<sup>55</sup> Recently, plasmid-mediated rRNA methyltransferases that confer high-level resistance to AGAs have been documented and reported in a number of pathogens including *Pseudomonas aeruginosa*, *Klebsiella pneumoniae*, *Escherichia coli*, *Serratia marcescens*, *Proteus mirabilis*, and *Acinetobacter baumannii*, indicating that further spread is likely.<sup>54, 56-63</sup>

## 2.6 Combatting Resistance

The immediate response to antibiotic resistance should be the reduction of both the overuse and misuse of these agents to limit the rate at which resistance is developed. Resistance to antibiotics should be anticipated and countermeasures against resistance mechanisms must be developed. To this end, modern medicinal chemistry has been extensively utilized to develop new compounds. This has led to a wealth of knowledge of primarily semisynthetic chemistry and structure-activity relationships (SARs).<sup>64</sup>

A product of these libraries, plazomicin (**2.9**) is a next-generation derivative of sisomicin (**2.10**). Plazomicin effectively avoids most AMEs through the combination of a hydroxyaminobutyric acid substituent at the 1-position of the 2-DOS and an ethanolamine at the 6'-position (**Figure 2.3**).<sup>30</sup> These added side chains likely add steric blockage, shielding the AGA from AMEs. While plazomicin activity is only affected by AAC(2')-I, like all of the other clinically relevant AGAs it is still blocked by both the G1405 and A1408 methyltransferases.<sup>30</sup> The example of plazomicin is proof that we have come far and that the abundant knowledge surrounding these compounds can be leveraged to generate new, improved AGAs. It is important to note that the challenges presented by methyltransferase activity are unlikely to be solved without access to derivatives with deeper structural changes. This observation leads us to the heart of this work; gaining synthetic access to structurally diverse AGAs.

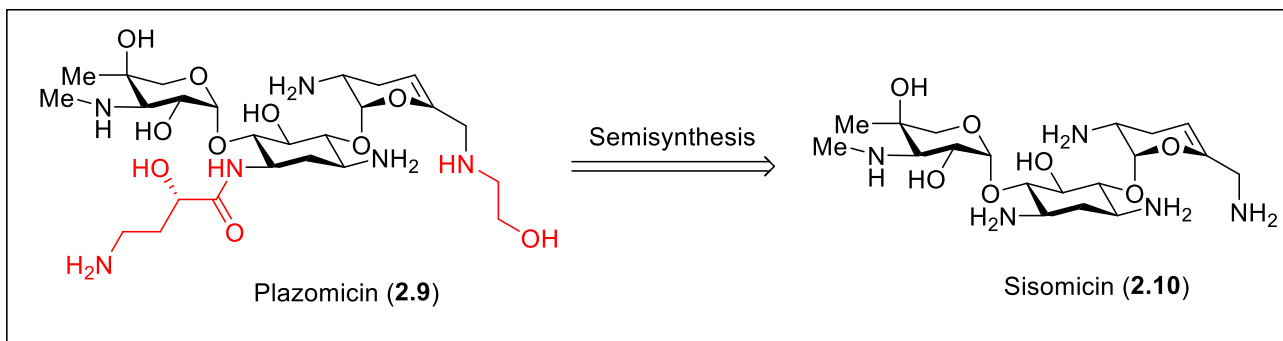


**Figure 2.3** Latest generation AGA plazomicin and parent sisomicin, structural improvements in red

## Chapter 3: Scaffold Design and Progress

### *3.1 Introduction*

In chapters one and two I introduced the discovery of antibiotics, the evolution of resistance to antibiotics, AGAs as potent bactericidal weapons, known resistance to AGAs, and how researchers have overcome this resistance in the next generation of AGAs. While semisynthetic efforts have proved fruitful in developing the latest generations of AGAs through sidechain and functional group manipulations, fully synthetic means are still required to probe deeper structural features. This idea is especially significant given the emerging threat of bacterial methylation resistance and the structural confines this pressure places on AGAs. The goal of this project has been to design and develop a chemical scaffold which provides access to the chemical space where these new AGAs reside.

### 3.2 Aminoglycoside Design Platform

The 4,5-AGA neomycin scaffold was chosen as a starting point for this work. While unaffected by G1405 methylation, the parent neomycin structure suffers from many AMEs. These AMEs are AAC(1), AAC(3), AAC(2'), APH(3'), ANT(4'), and AAC(6'). Neomycin family AGAs are also susceptible to A1408 methylation which may become an increasing concern in the future.

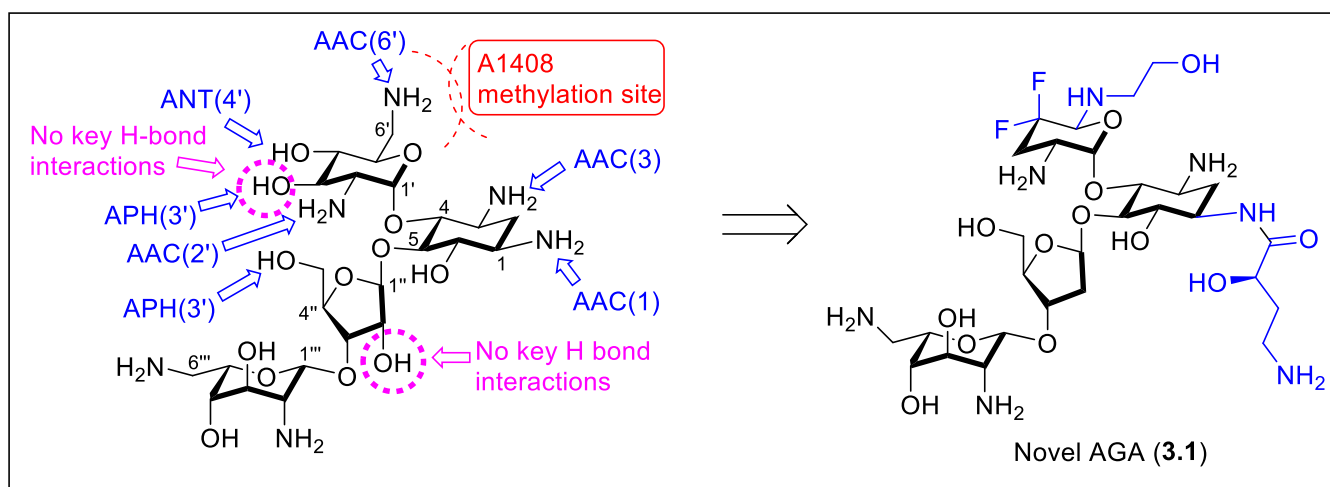


**Figure 3.1** Challenges to parent neomycin scaffold (left) and novel AGA (**3.1**) with improvements

Key modifications were designed around the current understanding of the literature surrounding AGAs. Drawing from the recent success of plazomicin, the design (**Figure 3.1**) features a 1-hydroxyaminobutyric acid and a 5'-ethanolamine side chain which should serve to sterically shield from AMEs. It was noticed that several of the hydroxyl groups were unnecessary for AGA activity yet remained targets for AMEs so the 2''- and 3''- alcohols were removed. This should add to the hydrophobic nature of the resultant AGA and in doing so increase the affinity of the electrostatic association involved in the uptake of AGA into the bacterial cell. Lastly, the 4'-alcohol was replaced by a *gem*-difluoromethylene bioisostere which should retain hydrogen bond donor capacity while removing the target of ANT(4'). Importantly, this approach is fully synthetic which means that once established, deeper structural changes will be possible. This should give our approach the adaptability to combat A1408 methylases, should they become more prevalent.

### 3.3 Synthetic Strategy

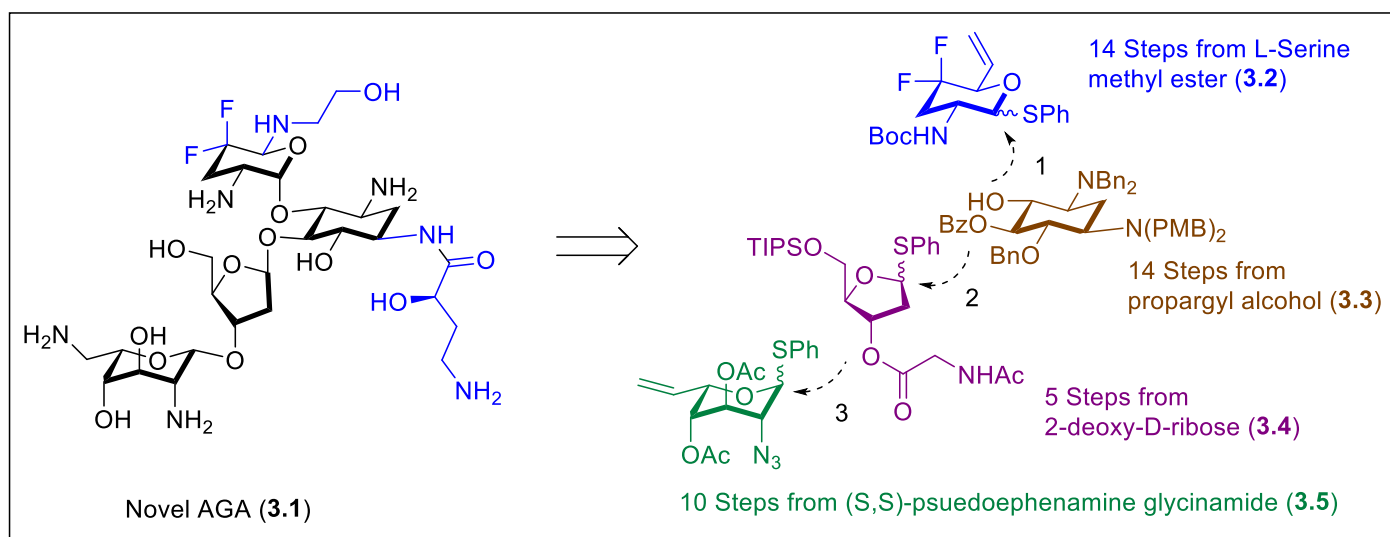


**Figure 3.2** Novel AGA (3.1) and retrosynthetic analysis to building blocks (3.2), (3.3), (3.4), and (3.5)

Having arrived at novel neomycin derived AGA (3.1), retrosynthetic analysis (**Figure 3.2**) traced back to four key building block sugars (3.2), (3.3), (3.4), and (3.5) which could be joined via glycosidic linkage. Importantly, fragments (3.2) and (3.5) possess alkenes as part of the design to facilitate the rapid development of analogs at sites directly impacted by rRNA methylation.

### 3.4 Synthesis of (3.4)<sup>65</sup>

Building block (3.4) starts from 2-deoxyribose which undergoes peracetylation with acetic anhydride and pyridine base to generate acetylated sugar (3.7). Following  $\text{BF}_3\text{OEt}_2$  mediated thioglycoside formation, sugar (3.8) undergoes saponification to generate (3.9). Triisopropylsilyl ether protection to (3.10) followed by carbonyldiimidazole mediated coupling with N-acetylglycine gave the 2-deoxyribose building block (3.4).

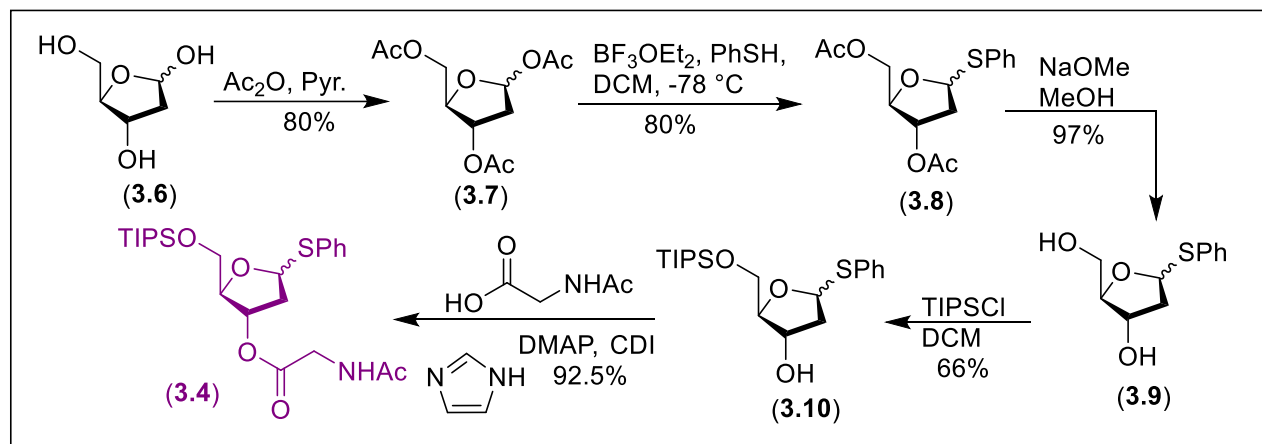


**Figure 3.3** Synthesis of 2-deoxyribose building block (3.4)

### 3.5 Synthesis toward (3.2)<sup>66-70</sup>

Building block (3.2) is a de novo sugar starting from L-serine methyl ester. Following the synthesis of Garner's aldehyde, N-butoxycarbonyl protection followed by oxazolidine formation with 2,2-dimethoxypropane gave methyl ester (3.12). Lithium aluminum hydride reduction to primary alcohol (3.13) with subsequent Swern oxidation gave aldehyde (3.14). This aldehyde then underwent a Corey-Fuchs reaction series to first generate dibromoalkene (3.15) which is primed to undergo Fritsch-Buttenberg-Weichell rearrangement in the presence of ethyl Grignard to give (3.16). Sonogashira coupling of this terminal alkyne to 2-bromofuran gave the disubstituted alkyne (3.17). Remaining in the route is the dihydrofluorination across this alkyne followed by ozonolysis of the furan and capture of the resultant carboxylate to the corresponding methyl ester (3.19). Following diisobutyl aluminum hydride reduction to aldehyde (3.20) asymmetric addition of vinyl Grignard following chiral zinc conditions pioneered by Noyori *et al.* should give allylic alcohol (3.21). Trifluoroacetic acid mediated ring opening of the oxazolidine should provide diol (3.22), which following Swern oxidation and in-situ cyclization can generate de novo sugar (3.23). Lastly, BF<sub>3</sub>OEt<sub>2</sub> mediated thioglycoside formation should provide building block (3.2).

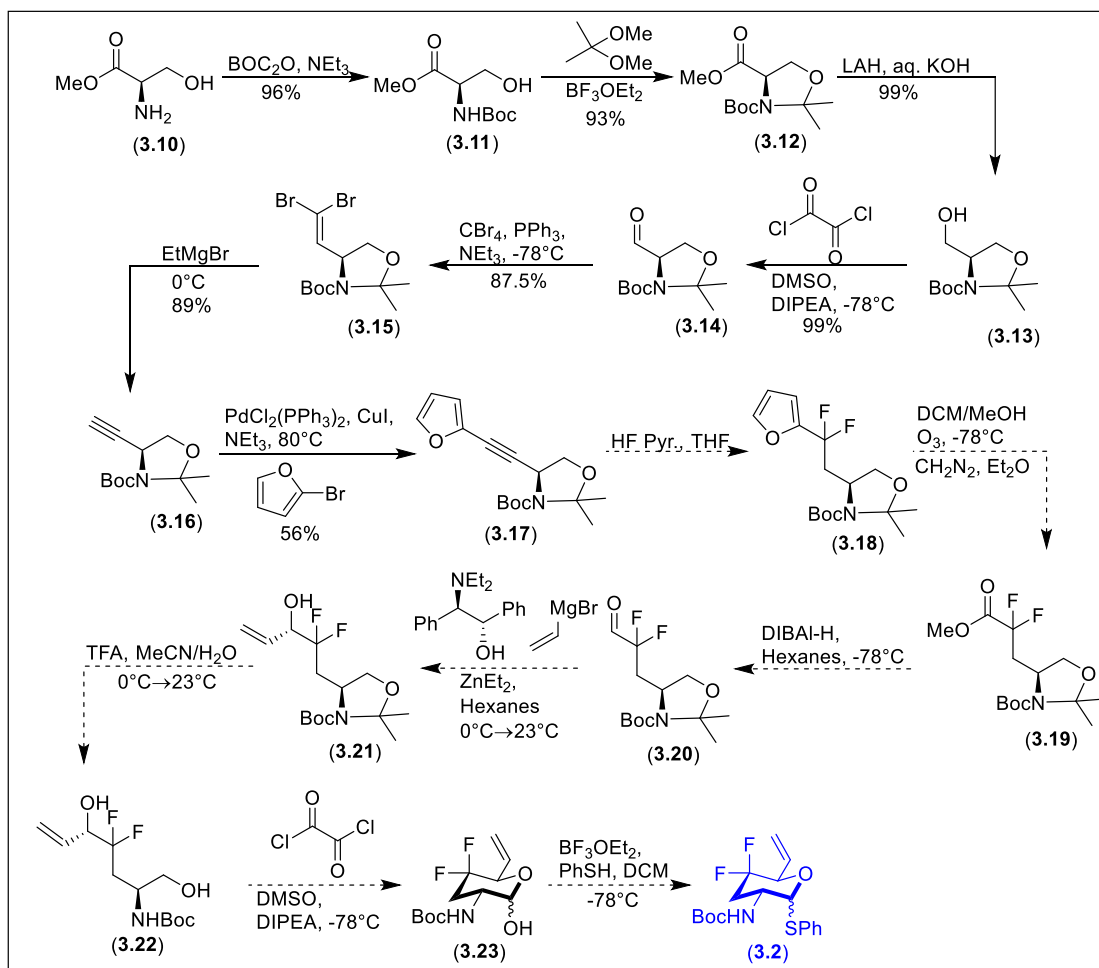


**Figure 3.4** Synthetic progress toward *gem*-difluoromethylene building block (3.2)



### 3.6 Synthetic Plan for (3.3)<sup>69-73</sup>

Synthesis toward (3.3) started with propargyl alcohol undergoing *tert*-butyldimethylsilyl ether protection to generate (3.25). Following this synthetic plan would generate the alkynyl anion upon exposure to *n*-butyl lithium and the disubstituted alkyne (3.26) upon capture with methyl chloroformate. Upon appending the proline derived chiral auxiliary from the Enders group to generate (3.27), tetrabutylammonium fluoride mediated butenolide formation should give (3.28). Upon activation by lithium hexamethyldisilazide can be trapped as (3.30) with *tert*-butyldiphenylsilyl chloride. Using highly similar work pioneered by the Schlessinger group as inspiration, the key Diels-Alder cyclization with diene (3.29) and mediated by triisopropoxy titanium chloride should give (3.31) after mild aqueous cleavage of chiral proline auxiliary. Reductive amination directed by the bridging oxygen should then give (3.33). Following Baeyer-Villiger oxidation to (3.34), deprotection of the silyl ether should collapse the bridging ring system as it did in Schlessinger's example to arrive at (3.35). Following another reductive amination, this time directed by the adjacent acetyl group, 2-DOS derivative (3.36) should be achieved. Benzoylation of the free alcohol followed by saponification of the acetyl group should give our orthogonally protected 2-DOS derivative (3.3).

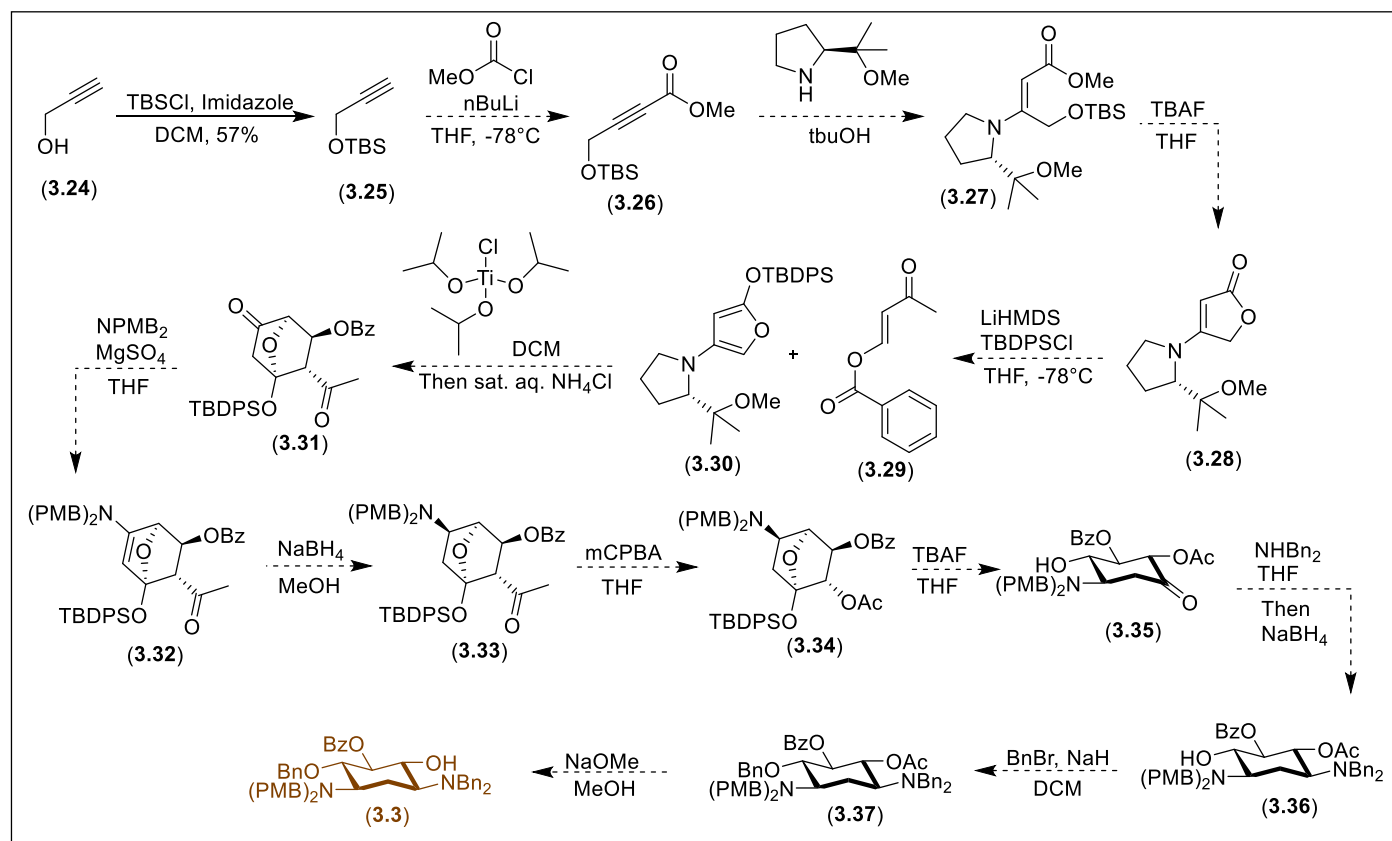


**Figure 3.5** Synthetic route to 2-DOS building block (3.3)

### 3.7 Synthetic Plan for (3.5)<sup>69, 70, 74</sup>

Synthetic route to (3.5) begins with (S,S)-pseudoephedrine glycinamide undergoing diastereoselective aldolization with (R)-glyceraldehyde acetonide to generate chiral aminoalcohol (3.39). Following cleavage of chiral auxiliary to (3.40) and esterification to (3.41), diazotransfer should give the  $\alpha$ -azide methyl ester (3.42). Tosic acid catalyzed migration of acetonide should reveal primary alcohol (3.43) which can undergo Dess-Martin periodane oxidation to resultant aldehyde (3.44). Chelate-controlled vinylation with divinylzinc gives allylic alcohol (3.45) which upon reduction to resultant aldehyde following diisobutyl aluminum hydride reduction can undergo *in situ* acid catalyzed acetonide cleavage and cyclization to de novo sugar (3.46). Peracetylation and the following BF<sub>3</sub>OEt<sub>2</sub> mediated thioglycoside formation should provide the last building block (3.5).

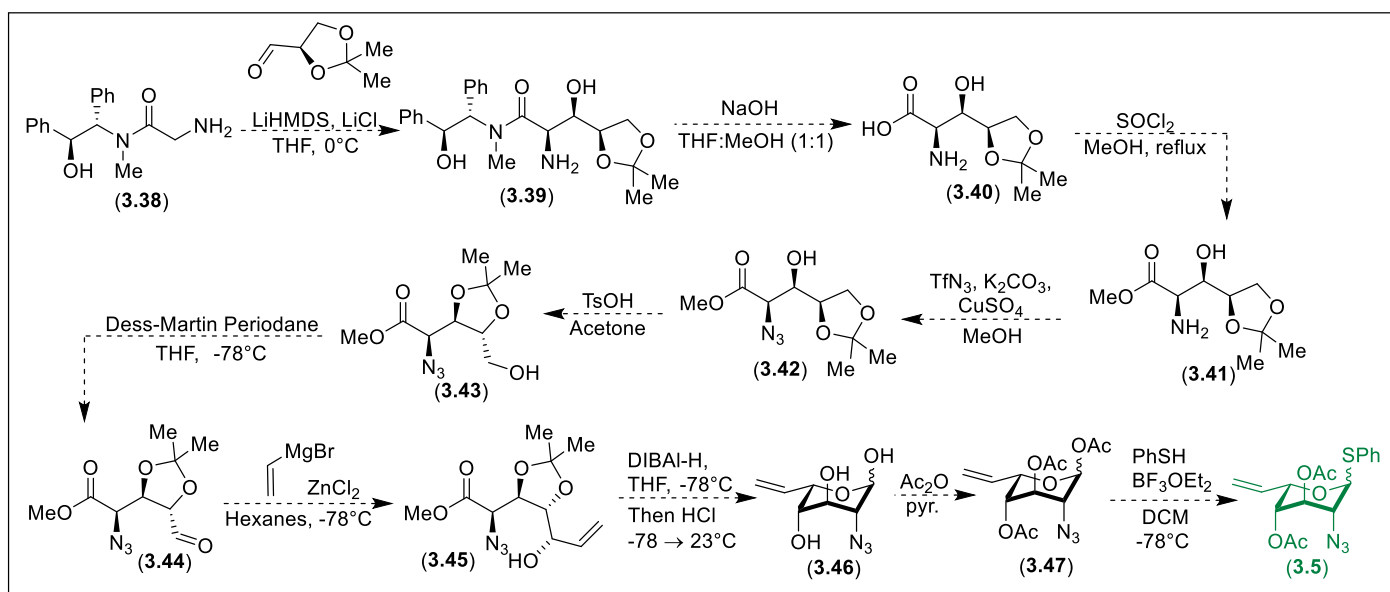


**Figure 3.6** Synthetic route to building block (3.5) from (S,S)-pseudoephedrine glycinamide

With all 4 key building blocks in hand, the final unification can commence. Starting with **(3.3)** and **(3.2)**, glycosylation following conditions described by Crich et al. is hypothesized to give the  $\alpha$ -linked pseudodisaccharide. Ozonolysis of the terminal alkene of **(3.2)** and reductive amination of the resultant aldehyde installs a protected ethanolamine side chain at the 6'-position. Ceric ammonium nitrate deprotection of the N-paramethoxybenzyl groups yields the resultant amine which is used to install the protected hydroxyaminobutyric acid side chain under basic conditions. Finally, saponification of the benzoyl ester reveals glycosylation acceptor **(3.48)**. Glycosylation with donor **(3.4)** should give the  $\beta$ -linked pseudotrisaccharide via anchimeric assistance from the N-acetylglycine side chain. Saponification of this N-acetylglycine side chain then reveals acceptor **(3.49)**. Once more utilizing conditions established by Crich et al., it is hypothesized that the  $\alpha$ -linked pseudotetrasaccharide can be achieved. Ozonolysis of the terminal alkene of the newly installed carbohydrate and reductive amination with dibenzylamine followed by a final saponification of the remaining acetyl groups should give **(3.50)**. The last deprotection steps of removing the silyl ether with tetrabutylammonium fluoride, acid catalyzed butoxycarbonyl deprotection, and global hydrogenation of the remaining protecting groups forges the desired novel 4,5-AGA **(3.1)**.

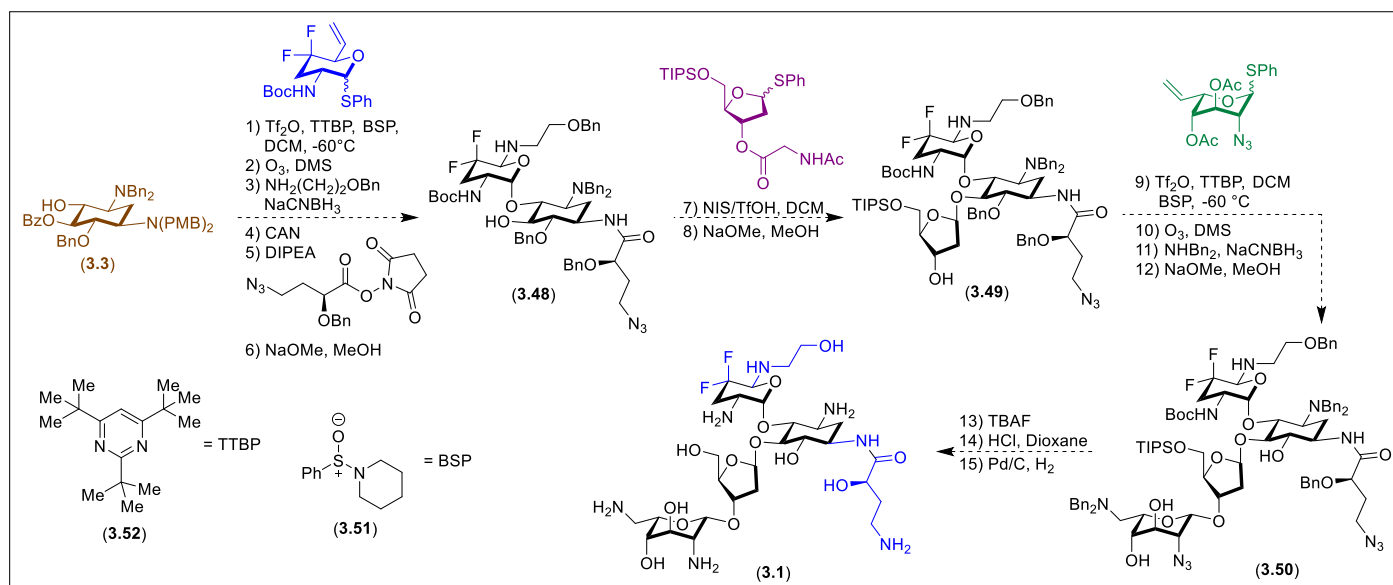


**Figure 3.7** Glycosylation strategy and late-stage manipulations toward novel AGA (**3.1**)

### *3.9 Conclusion*

The design and synthesis of a synthetic platform toward novel 4,5-AGAs has been initiated. To date, building block (3.4) has been made, and significant progress has been made toward building block (3.2). Continuation of this project should focus on the realization of the remaining 3 carbohydrate units and unification to the desired (3.1). Once realized, the platform should be used to expand and probe the new chemical space for AGAs which have increased potential, especially in response to emerging resistance.

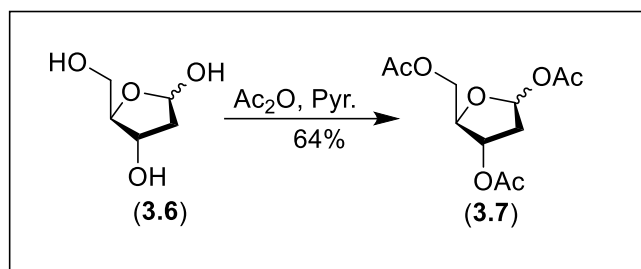
## *General Methods*

Commercial reagents were used as received. Anhydrous solvents were taken from an MBRAUN solvent purification system (MB SPS) and stored over 4 Å or 3 Å molecular sieves. All moisture-sensitive reactions were performed in flame- or oven-dried round bottom flasks under an argon atmosphere. All air- or moisture-sensitive liquids were transferred via oven-dried stainless-steel syringes or cannula. Reaction temperatures were monitored and controlled via thermocouple thermometer and corresponding hot plate stirrer. Flash column chromatography was performed as described by Still et. al. using silica gel 230-400 mesh. Analytical thin-layer chromatography (TLC) was performed on glass-backed Silica gel 60 F<sub>254</sub> plates (EMD/Merck KGaA) and visualized using UV, cerium ammonium molybdate stain, and anisaldehyde stain.

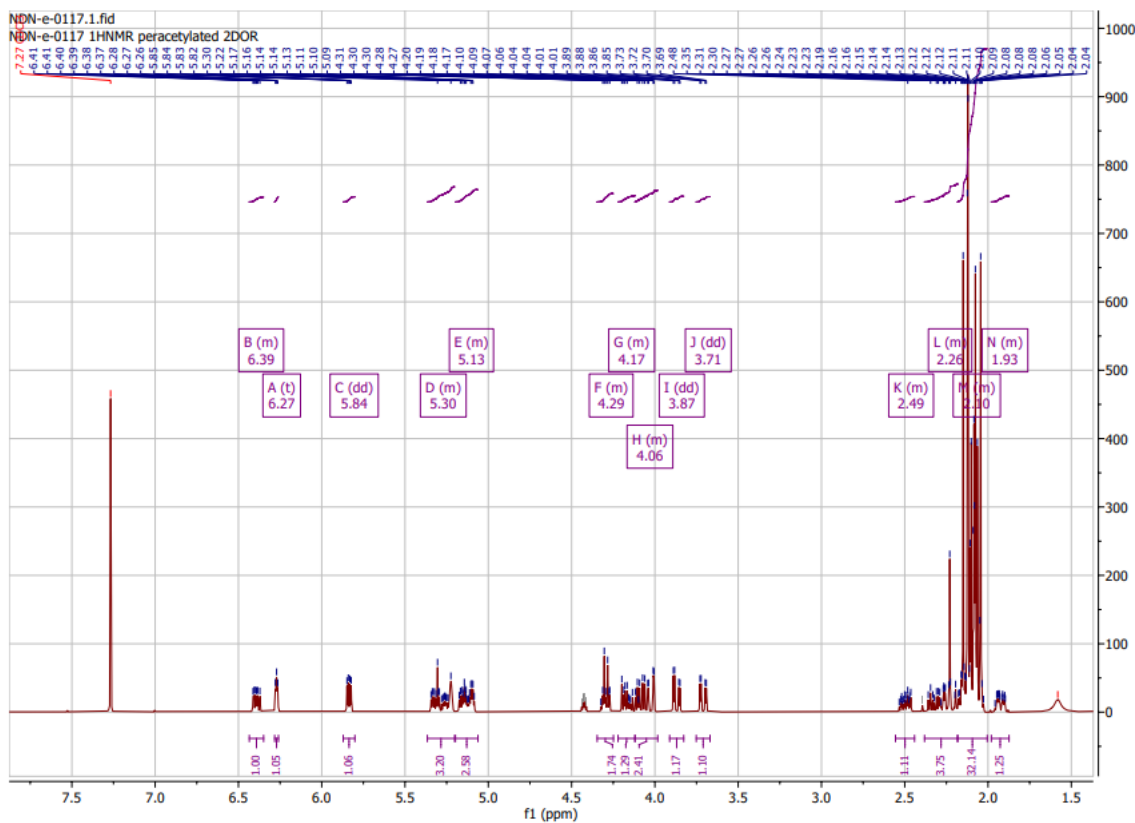
## *Instrumentation*

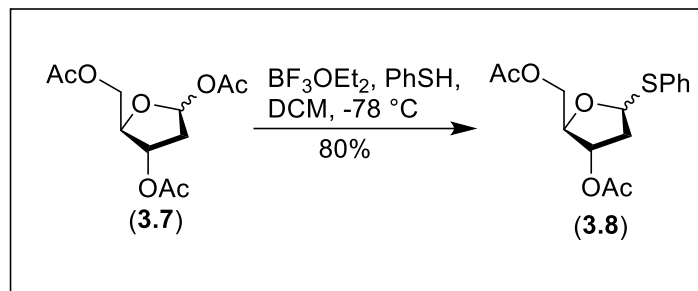
<sup>1</sup>H NMR spectra were obtained on a Bruker 400 or 600 MHz spectrometer with reporting relative to deuterated solvent signals. <sup>1</sup>H NMR spectral data are presented as follows: chemical shifts ( $\delta$  ppm), multiplicity (s=singlet, d=doublet, dd=doublet of doublets, t=triplet, q=quartet, p=pentet, m=multiplet, br=broad, app=apparent), coupling constants (J in Hz), integration, proton assignment. Deuterated chloroform was calibrated to 7.26 ppm. Deuterated methanol was calibrated to 3.31 ppm. <sup>13</sup>C NMR spectra were obtained on a Bruker 100 MHz or 150 MHz spectrometer with reporting relative to deuterated solvent signals. <sup>13</sup>C NMR spectral data are presented as follows: chemical shifts ( $\delta$  ppm), carbon assignment. Deuterated chloroform was calibrated to 77.16 ppm. Deuterated methanol was calibrated to 49.0 ppm. Proton and carbon assignments were made with the aid of 2D NMR techniques (COSY, HSQC).

## Synthetic Procedures

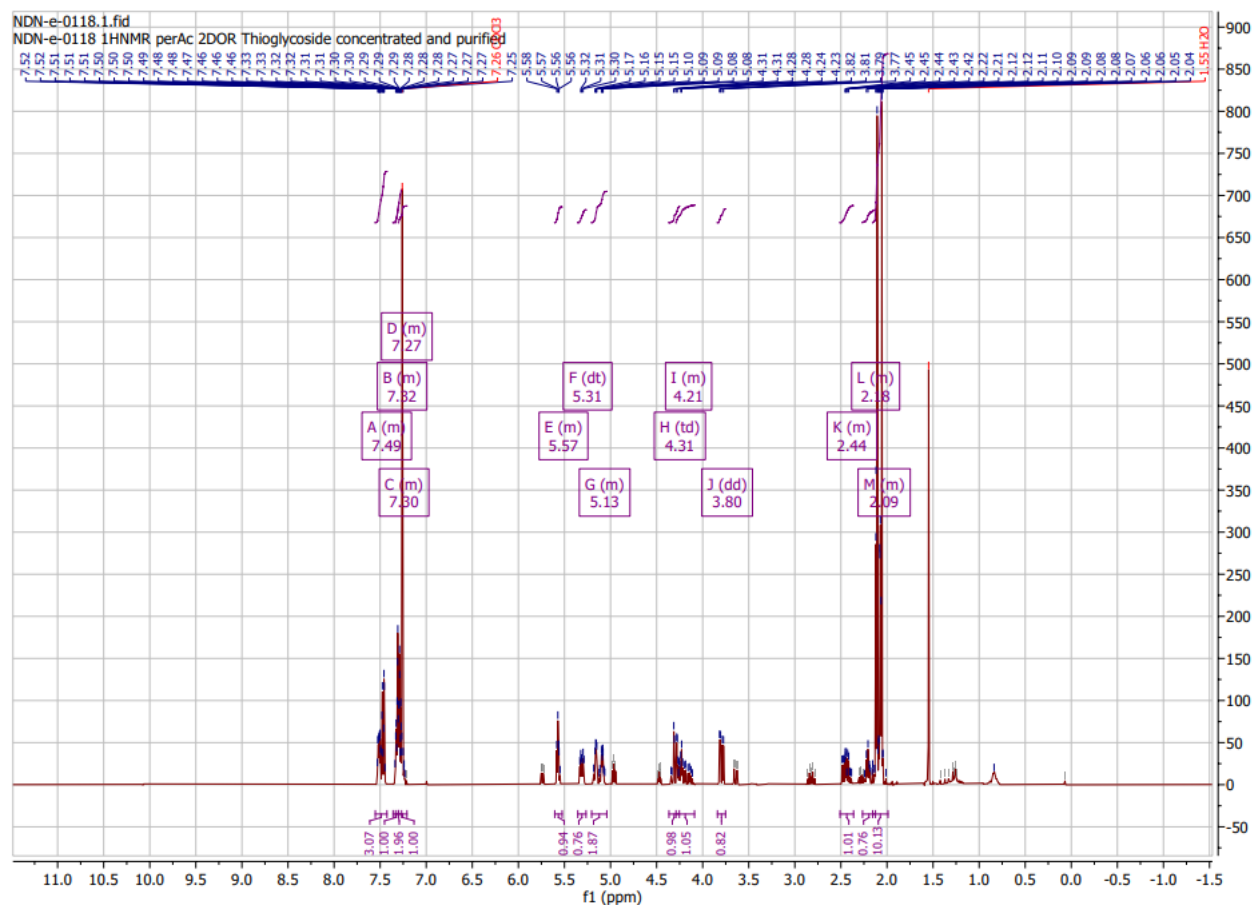


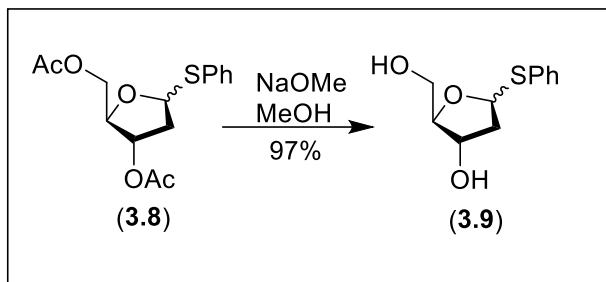
5-(acetoxymethyl)tetrahydrofuran-2,4-diyl diacetate: To an oven dried 1L flask and stir bar under argon was added 2-deoxyribose (1.0eq, 10g, 75mmol) and pyridine (200mL). Reaction was cooled to 0°C and stirred for 15 minutes before beginning addition of acetic anhydride (6eq, 42mL, 0.45mol) dropwise. After addition reaction was warmed to room temperature and stirred for 12 hours until TLC showed full conversion of starting material. Reaction was diluted with EtOAc and cooled to 0°C over 15 minutes. Mixture was then transferred to separatory funnel and washed 12 times with 80mL portions of 1N HCl. Product 5-(acetoxymethyl)tetrahydrofuran-2,4-diyl diacetate was purified via column chromatography (12.5g, 64%) and verified via <sup>1</sup>H NMR as a mixture of anomers. <sup>1</sup>H NMR (400 MHz, CDCl<sub>3</sub>) δ 6.43 – 6.35 (m, 1H), 6.27 (t, J = 2.8 Hz, 1H), 5.84 (dd, J = 6.8, 3.2 Hz, 1H), 5.37 – 5.20 (m, 3H), 5.20 – 5.06 (m, 3H), 4.35 – 4.25 (m, 2H), 4.22 – 4.12 (m, 1H), 4.12 – 3.98 (m, 2H), 3.87 (dd, J = 13.0, 2.8 Hz, 1H), 3.71 (dd, J = 12.5, 2.6 Hz, 1H), 2.56 – 2.44 (m, 1H), 2.38 – 2.18 (m, 4H), 2.18 – 2.00 (m, 32H), 1.98 – 1.87 (m, 1H).<sup>76</sup>





(3-acetoxy-5-(phenylthio)tetrahydrofuran-2-yl)methyl acetate: To an oven dried 100mL flask and stirbar under argon was added 5-(acetoxymethyl)tetrahydrofuran-2,4-diyl diacetate (1.0eq, 1.00g, 3.84mmol) and dichloromethane (50mL). Reaction vessel was cooled to  $-78^\circ\text{C}$ , color is clear. Thiophenol (1.0eq, 423mg, 3.84mmol) from 1M stock solution added dropwise.  $\text{BF}_3\text{OEt}_2$  added dropwise and solution stirred for 2 hours at  $-78^\circ\text{C}$ . Color is clear. Solution then warmed to  $23^\circ\text{C}$ . Solution changed from clear to pink and then to begin to change to yellow. Quenched with sat. aq.  $\text{NaHCO}_3$  solution. Extracted with EtOAc 3 times with 100mL portions. Dried over  $\text{Na}_2\text{SO}_4$  and concentrated in vacuo. Purified via column chromatography to yield (3-acetoxy-5-(phenylthio)tetrahydrofuran-2-yl)methyl acetate (0.96g, 80%), a mixture of anomers, verified by  $^1\text{H NMR}$ .  $^1\text{H NMR}$  (400 MHz,  $\text{CDCl}_3$ )  $\delta$  7.55 – 7.43 (m, 3H), 7.36 – 7.30 (m, 1H), 7.33 – 7.27 (m, 2H), 7.30 – 7.21 (m, 1H), 5.61 – 5.53 (m, 1H), 5.31 (dt,  $J = 10.3, 3.8$  Hz, 1H), 5.20 – 5.04 (m, 2H), 4.31 (td,  $J = 12.2, 2.9$  Hz, 1H), 4.29 – 4.09 (m, 1H), 3.80 (dd,  $J = 12.6, 4.5$  Hz, 1H), 2.51 – 2.36 (m, 1H), 2.27 – 2.13 (m, 1H), 2.16 – 1.99 (m, 10H).<sup>65</sup>

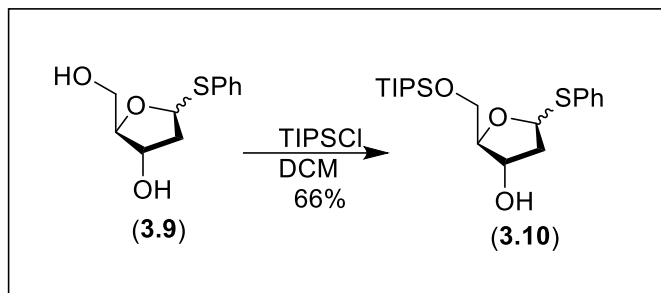




2-(hydroxymethyl)-5-(phenylthio)tetrahydrofuran-3-ol: To an oven dried 500mL flask and stir bar under argon was added substrate (1.0eq, 9.5g, 31mmol) and anhydrous MeOH (200mL). 1M NaOMe solution (3eq, 93mL, 93mmol) was added. pH = 12. Solution stirred 12 hours at which TLC showed consumption of starting material. Color is yellow. DOWEX resin added to neutralize. pH = 7. Filtered and concentrated in vacuo to yield 2-(hydroxymethyl)-5-(phenylthio)tetrahydrofuran-3-ol (6.7g, 97%). Color = vibrant red. <sup>1</sup>H NMR showed mixture of anomers. <sup>1</sup>H NMR (400 MHz, MeOD) δ 7.54 – 7.41 (m, 3H), 7.35 – 7.16 (m, 4H), 5.48 (t, J = 4.7 Hz, 1H), 4.27 – 3.88 (m, 2H), 3.87 – 3.45 (m, 3H), 2.30 (ddd, J = 13.4, 9.1, 4.3 Hz, 1H), 2.21 – 1.96 (m, 1H), 1.99 – 1.87 (m, 1H).<sup>65</sup>

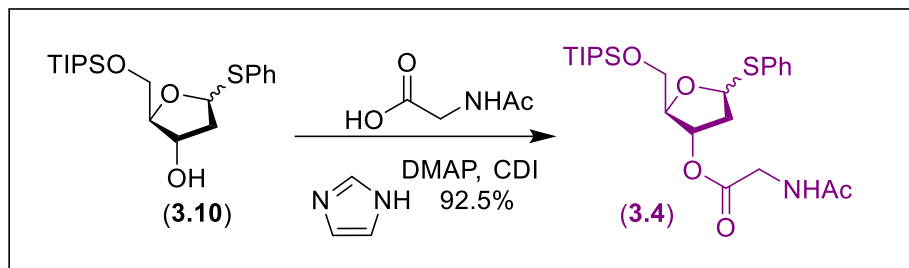




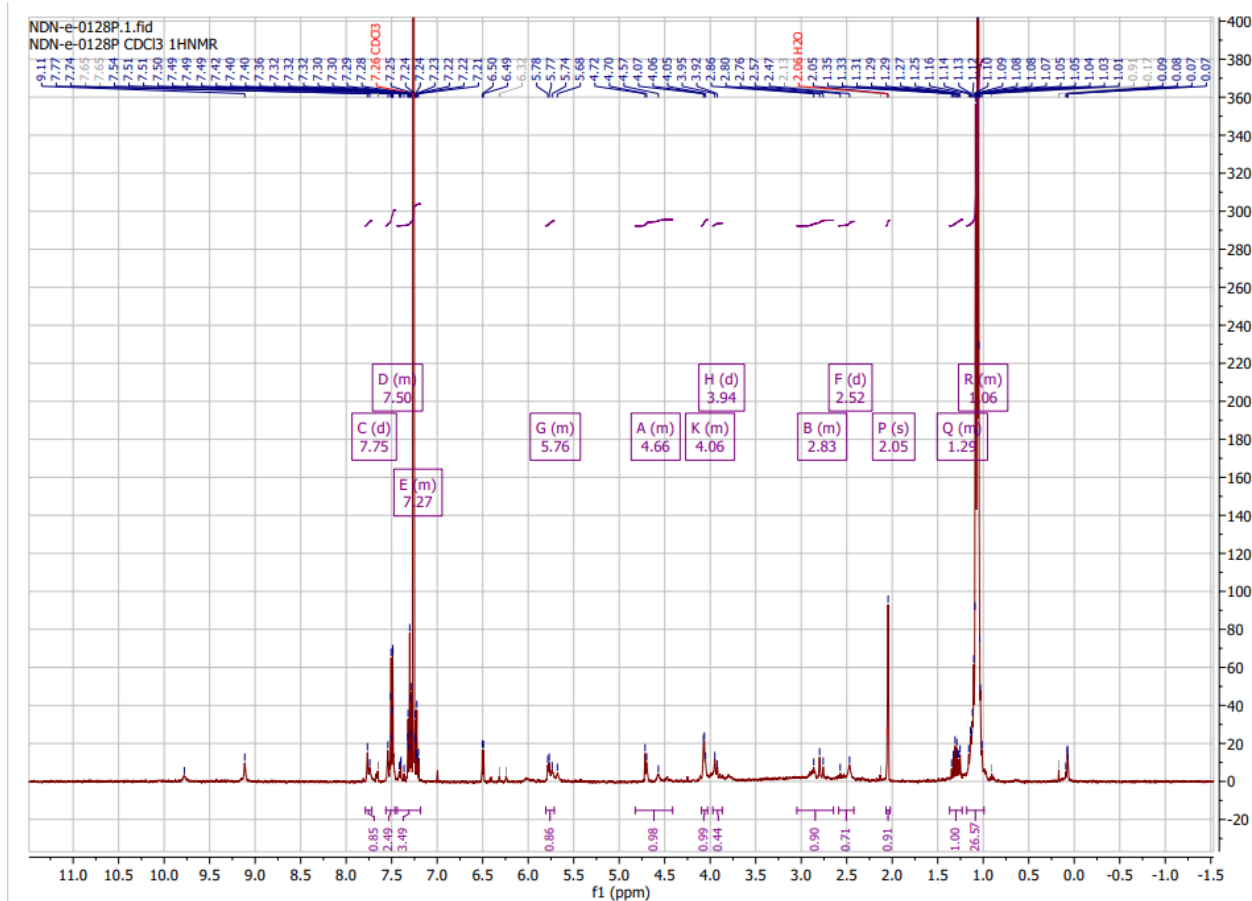


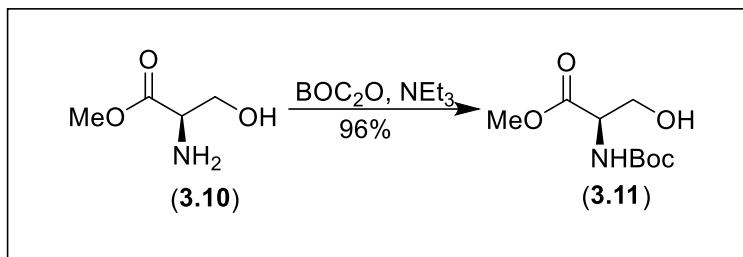
5-(phenylthio)-2-(((triisopropylsilyloxy)methyl)tetrahydrofuran-3-ol: To an 500mL oven dried flask and stir bar under argon was added 2-(hydroxymethyl)-5-(phenylthio)tetrahydrofuran-3-ol (1.0eq, 5.61g, 24.8mmol), dichloromethane (200mL), and imidazole (1.1eq, 1.86g, 27.3mmol). Color = yellow. Solution stirred for 15 minutes and then triisopropylsilylchloride was added and color changed to milky. Solution stirred for 16 hours before TLC showed conversion. Reaction was diluted with dichloromethane and transferred to a separatory funnel where it was washed with DI H<sub>2</sub>O 50mL and extracted with 3 100mL portions of dichloromethane. Extracts were dried over Na<sub>2</sub>SO<sub>4</sub> and concentrated in vacuo before being purified via column chromatography to yield 5-(phenylthio)-2-(((triisopropylsilyloxy)methyl)tetrahydrofuran-3-ol (4.70g, 50%) mixture of anomers verified via <sup>1</sup>HNMR. <sup>1</sup>H NMR (400 MHz, CDCl<sub>3</sub>) δ 7.53 – 7.45 (m, 4H), 7.37 – 7.26 (m, 5H), 7.22 (t, J = 7.3 Hz, 1H), 5.58 (dd, J = 9.6, 6.3 Hz, 1H), 5.14 – 4.97 (m, 3H), 4.91 – 4.79 (m, 1H), 4.76 (d, J = 8.5 Hz, 1H), 4.25 – 4.02 (m, 2H), 3.88 (d, J = 13.8 Hz, 1H), 2.79 – 2.63 (m, 1H), 1.92 (ddd, J = 15.8, 9.6, 3.1 Hz, 1H), 1.26 (s, 0H), 1.07 (d, J = 11.0 Hz, 0H), 0.84 (s, 1H).<sup>65</sup>



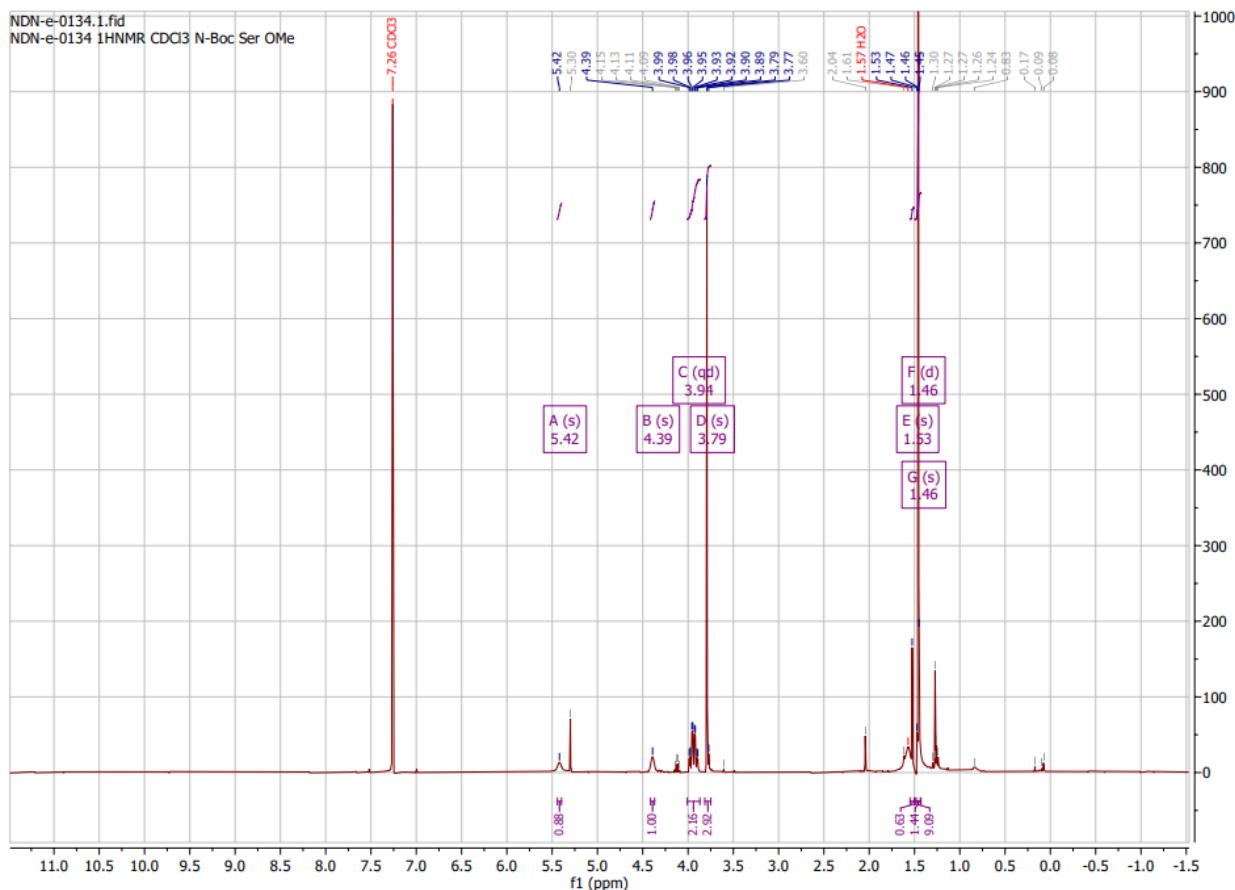


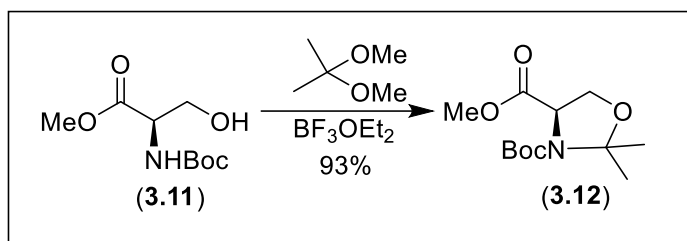
5-(phenylthio)-2-(((triisopropylsilyl)oxy)methyl)tetrahydrofuran-3-yl acetylglycinate: To an oven dried 250mL flask and stir bar under argon was added 5-(phenylthio)-2-(((triisopropylsilyl)oxy)methyl)tetrahydrofuran-3-ol (1.0eq, 1.70g, 4.44mmol), dichloromethane (100mL), and N-acetylglycine (1.3eq, 676mg, 5.78mmol). DMAP (5 mol%, 27.1mg, 0.222mmol) and CDI (1.3eq, 937mg, 5.78mmol) were added and the solution was stirred vigorously for 12 hours. Color = milky white. After conversion shown on TLC, the resultant solution was diluted with dichloromethane, quenched with sat. aq. NaHCO<sub>3</sub> solution. Mixture was moved to a separatory funnel where it was extracted with 3 portions of 100 mL dichloromethane. Extracts were dried over Na<sub>2</sub>SO<sub>4</sub> and concentrated in vacuo. Concentrate was purified via column chromatography to yield 5-(phenylthio)-2-(((triisopropylsilyl)oxy)methyl)tetrahydrofuran-3-yl acetylglycinate (1.98g, 92.5%) verified via <sup>1</sup>H NMR. <sup>1</sup>H NMR (400 MHz, CDCl<sub>3</sub>) δ 7.75 (d, J = 10.3 Hz, 1H), 7.56 – 7.46 (m, 2H), 7.44 – 7.18 (m, 3H), 5.81 – 5.71 (m, 1H), 4.82 – 4.41 (m, 1H), 4.10 – 4.03 (m, 1H), 3.94 (d, J = 10.9 Hz, 0H), 3.05 – 2.65 (m, 1H), 2.52 (d, J = 41.1 Hz, 1H), 2.05 (s, 1H), 1.37 – 1.23 (m, 1H), 1.18 – 0.99 (m, 27H).<sup>65</sup>



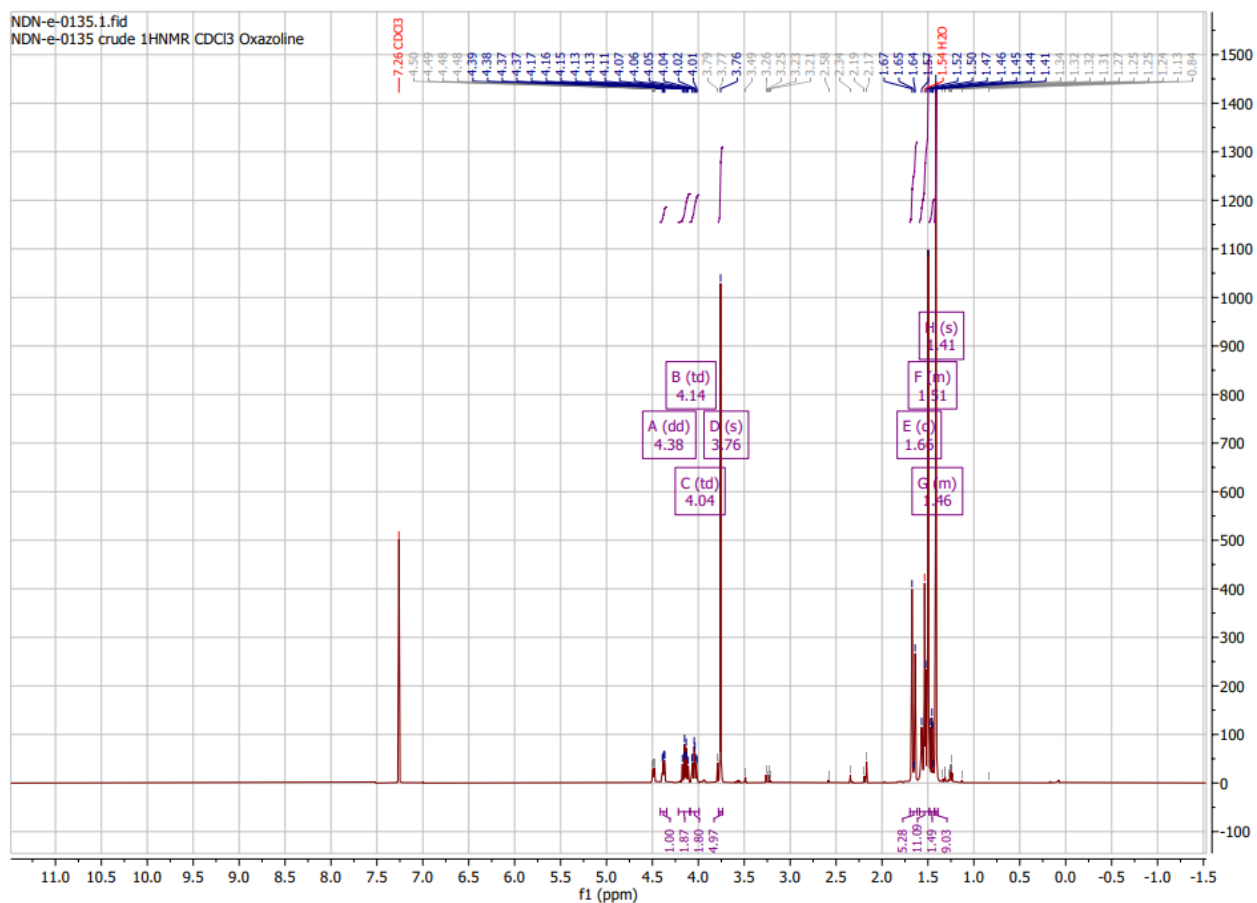


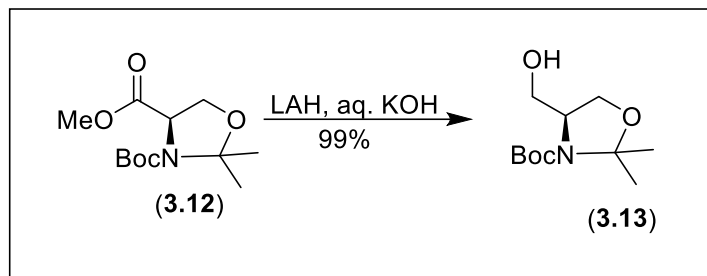
methyl (tert-butoxycarbonyl)-L-serinate: To an oven dried 1L flask and stir bar under argon fitted with a drop addition funnel was added methyl L-serinate--13-chlorane 1:1 (1.00eq, 15g, 95mmol), tetrahydrofuran (300mL), and triethylamine (2.10eq, 28mL, 0.2 mol) to main vessel. Tetrahydrofuran (100mL) and di-tert-butyl dicarbonate (1.00eq, 22mL, 95mmol) was added to drop addition funnel. Solution was cooled to 0°C and stirred for 15 minutes then dropwise addition proceeded after which reaction was warmed to 23°C and stirred for 12 hours. At this point mixture was heated to 50°C for 3 hours before cooling, concentrating in vacuo, and washing with sat. aq.  $\text{NaHCO}_3$ . Mixture was transferred to a separatory funnel and extracted with ether in 3 200mL portions. Extracts were dried over  $\text{Na}_2\text{SO}_4$  and concentrated in vacuo to yield methyl (tert-butoxycarbonyl)-L-serinate (20.3g, 97%) verified via  $^1\text{H NMR}$ .  $^1\text{H NMR}$  (400 MHz,  $\text{CDCl}_3$ )  $\delta$  5.42 (s, 1H), 4.39 (s, 1H), 3.94 (qd,  $J = 11.2, 3.8$  Hz, 2H), 3.79 (s, 3H), 1.53 (s, 1H), 1.46 (d,  $J = 8.7$  Hz, 1H), 1.46 (s, 9H).<sup>67</sup>



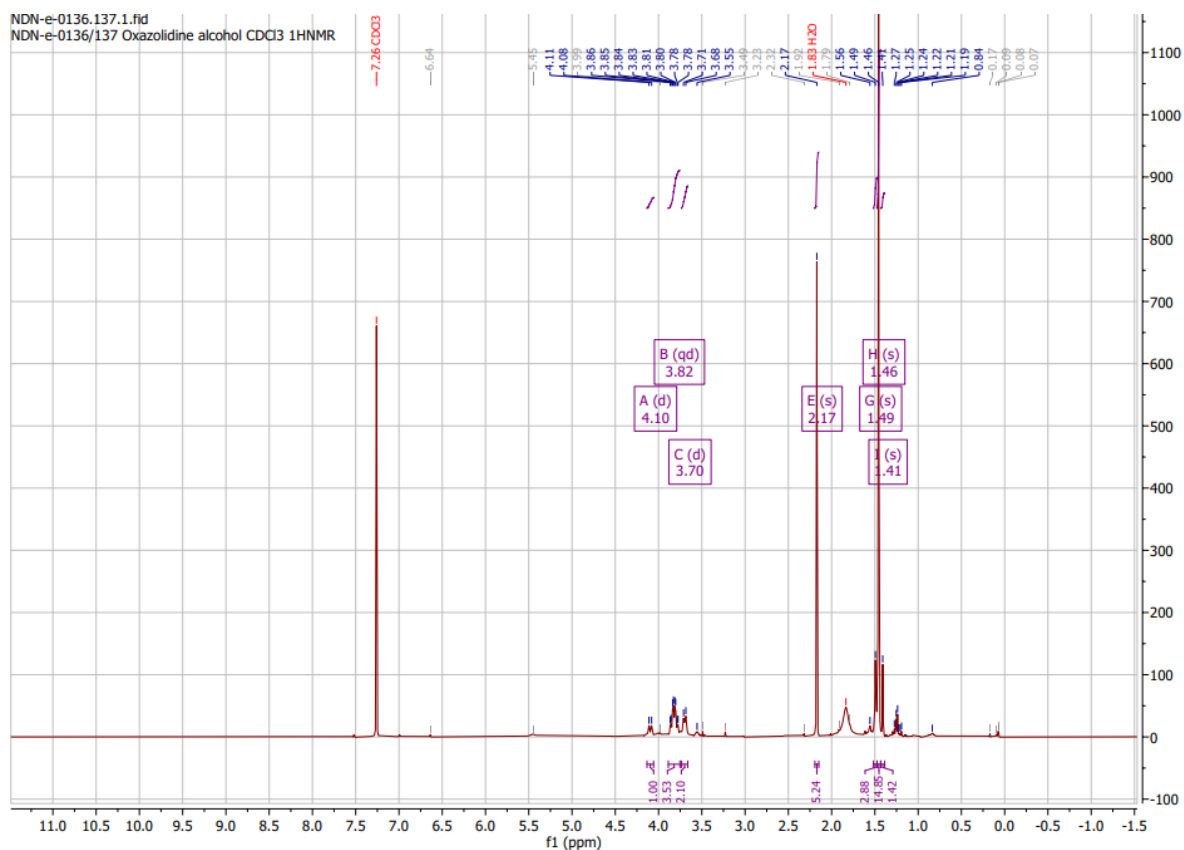


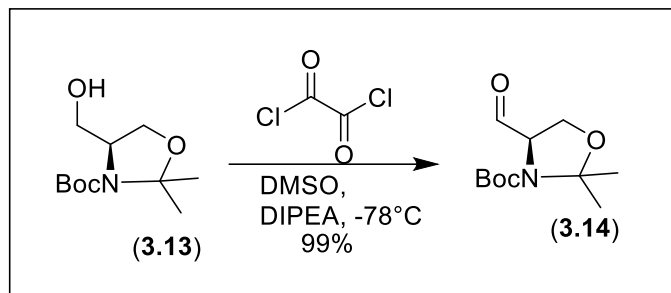
3-(tert-butyl) 4-methyl (S)-2,2-dimethyloxazolidine-3,4-dicarboxylate: To a an oven dried 1L flask and stir bar under argon was methyl (tert-butoxycarbonyl)-L-serinate (1.00eq, 20.0g, 91.2mmol), 2,2-dimethoxypropane (9.00eq, 101mL, 821mmol), and anhydrous acetone (200mL). Reaction was cooled to 0°C and stirred for 15 minutes.  $\text{BF}_3\text{OEt}_2$  (0.1eq, 1.29g, 9.12mmol) was added dropwise and color turned orange. Left stirring for 2 hours until TLC showed completion. Reaction was quenched with triethylamine (2.2mL) and concentrated in vacuo. The resultant was washed with sat. aq.  $\text{NaHCO}_3$  solution and extracted with 3 portions of 200mL ether. Extracts were dried over  $\text{Na}_2\text{SO}_4$  and concentrated in vacuo to give 3-(tert-butyl) 4-methyl (S)-2,2-dimethyloxazolidine-3,4-dicarboxylate (22.0g, 93%) verified via  $^1\text{H}$ NMR.  $^1\text{H}$  NMR (400 MHz,  $\text{CDCl}_3$ )  $\delta$  4.38 (dd,  $J = 7.0, 3.1$  Hz, 1H), 4.14 (td,  $J = 9.1, 6.9$  Hz, 2H), 4.04 (td,  $J = 9.5, 2.9$  Hz, 2H), 3.76 (s, 5H), 1.66 (d,  $J = 13.6$  Hz, 5H), 1.59 – 1.48 (m, 11H), 1.48 – 1.43 (m, 1H), 1.41 (s, 9H).<sup>67</sup>



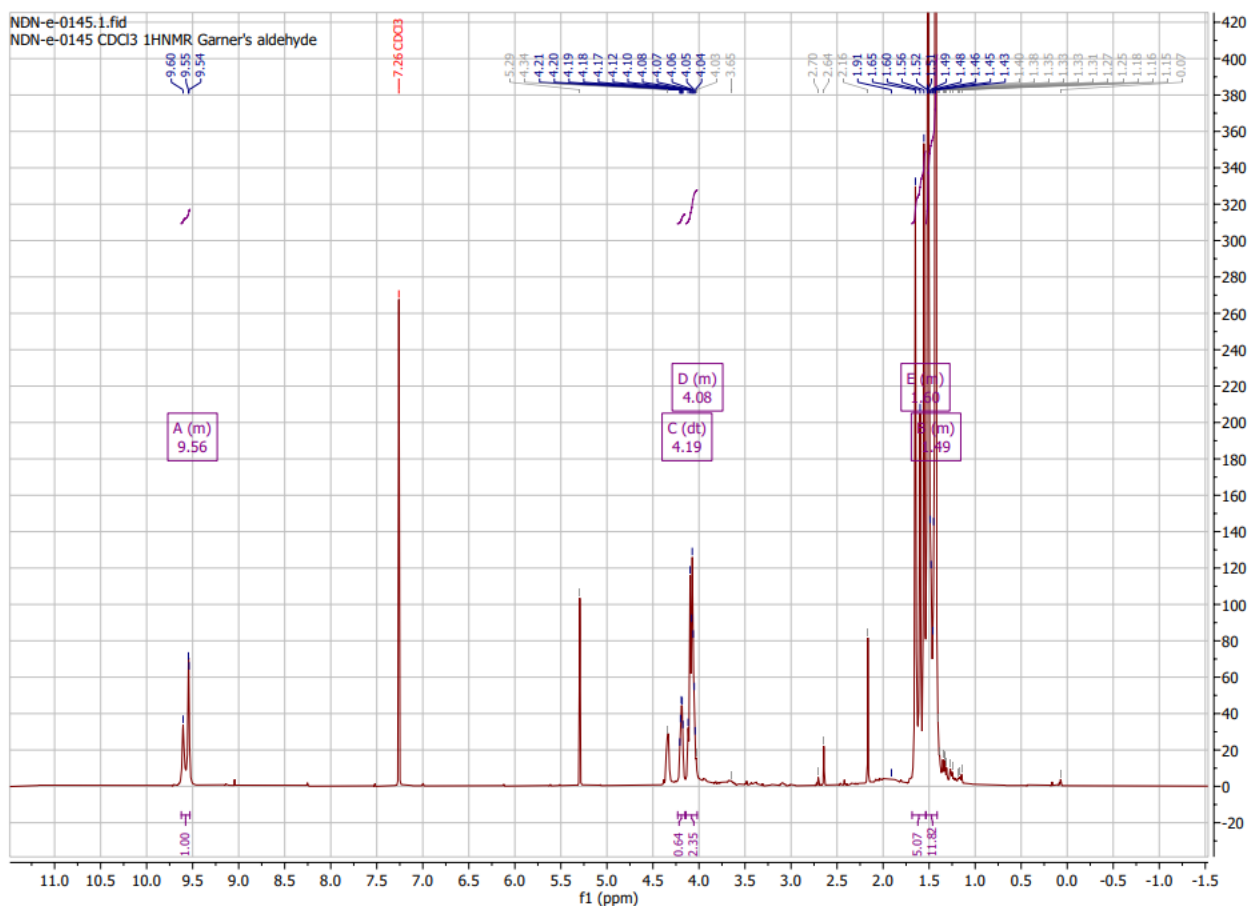


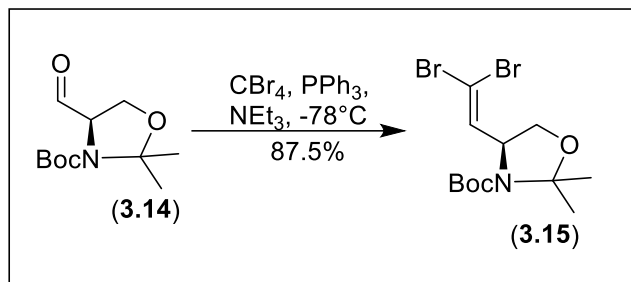
tert-butyl (R)-4-(hydroxymethyl)-2,2-dimethyloxazolidine-3-carboxylate: To an oven dried 100mL flask and stir bar under argon was added 3-(tert-butyl) 4-methyl (S)-2,2-dimethyloxazolidine-3,4-dicarboxylate (1.00eq, 2.00g, 7.71mmol) and tetrahydrofuran (40mL). Solution was cooled to 0°C and stirred for 15 minutes. Lithium aluminum hydride 2.4M solution (1.50eq, 4.82mL, 11.6mmol) was added dropwise and solution stirred another 10 minutes before warming to 23°C. Solution stirred for 20 minutes before TLC showed completion at which point solution was cooled to 0°C and 10% aq KOH solution (5mL) was added dropwise and mixture was warmed to 23°C and stirred for 1 more hour at which point it was filtered through a pad of celite and washed with ether in 3 60mL portions. This filtrate was moved to a separatory funnel where it was washed with aq. Wash and extraction with ether in 3 60mL portions gave extracts which were dried over Na<sub>2</sub>SO<sub>4</sub> and concentrated in vacuo to give crystalline tert-butyl (R)-4-(hydroxymethyl)-2,2-dimethyloxazolidine-3-carboxylate (1.78g, 99.8%) verified via <sup>1</sup>HNMR. <sup>1</sup>H NMR (400 MHz, CDCl<sub>3</sub>) δ 4.10 (d, J = 12.2 Hz, 1H), 3.82 (qd, J = 11.1, 3.9 Hz, 4H), 3.70 (d, J = 10.6 Hz, 2H), 2.17 (s, 5H), 1.49 (s, 3H), 1.46 (s, 15H), 1.41 (s, 1H).<sup>67</sup>



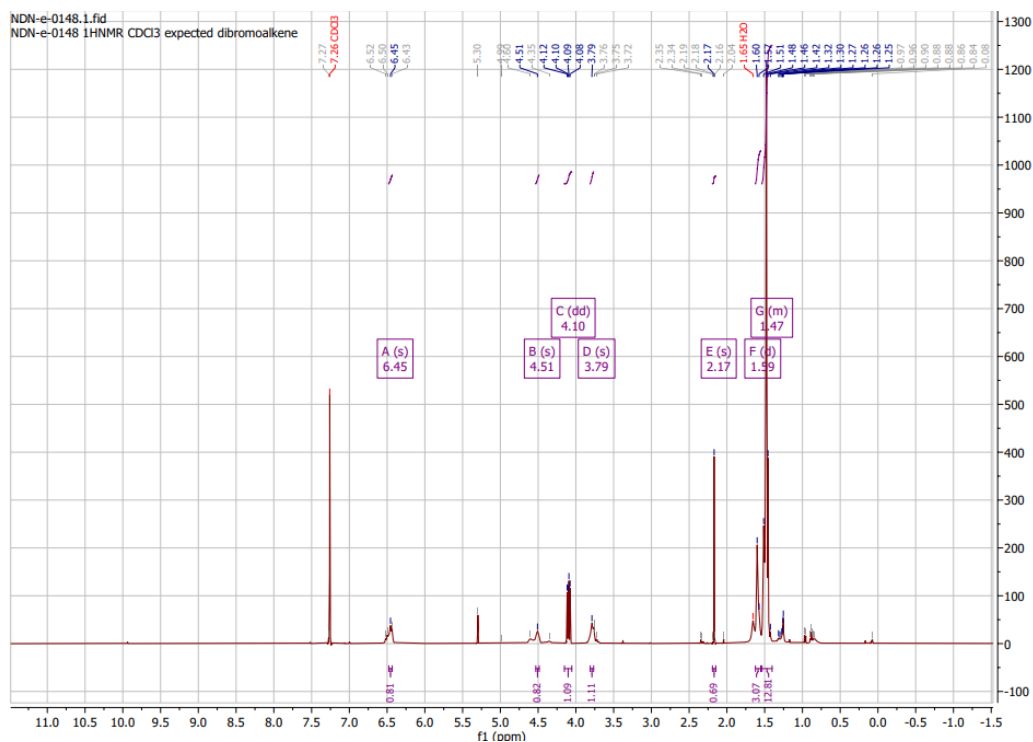


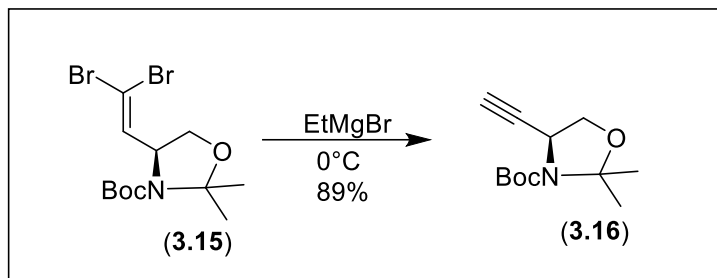
tert-butyl (S)-4-formyl-2,2-dimethyl-1-oxazolidinone-3-carboxylate: To an oven dried 500mL 2 neck flask and stir bar with fitted thermometer attachment, all under argon was added oxalyl chloride (1.5eq, 4.8mL, 56mmol), dichloromethane (150mL) and the liquid was cooled to  $-78^\circ\text{C}$ . Internal temperature =  $-78^\circ\text{C}$ . DMSO (3.00eq, 8.0mL, 0.11mol) was added dropwise and the mixture was warmed to an internal  $-60^\circ\text{C}$ . Tert-butyl (R)-4-(hydroxymethyl)-2,2-dimethyl-1-oxazolidinone-3-carboxylate (1.0eq, 8.70g, 38mmol) was added dropwise and the mixture was warmed to an internal  $-45^\circ\text{C}$  and stirred for 15 minutes at which point DIPEA (6.0eq, 39mL, 0.23mol) was added dropwise and color became clear. The resultant solution was warmed to  $0^\circ\text{C}$  and extracted from a chilled 1N HCl wash with dichloromethane in 3 150mL portions. The extracts were dried over  $\text{Na}_2\text{SO}_4$  and concentrated in vacuo to give tert-butyl (S)-4-formyl-2,2-dimethyl-1-oxazolidinone-3-carboxylate (8.57g, 99%) verified by  $^1\text{H NMR}$ .  $^1\text{H NMR}$  (400 MHz,  $\text{CDCl}_3$ )  $\delta$  9.62 – 9.53 (m, 1H), 4.19 (dt,  $J = 6.6, 3.2$  Hz, 1H), 4.14 – 4.02 (m, 2H), 1.68 – 1.54 (m, 5H), 1.53 – 1.41 (m, 12H).<sup>67</sup>



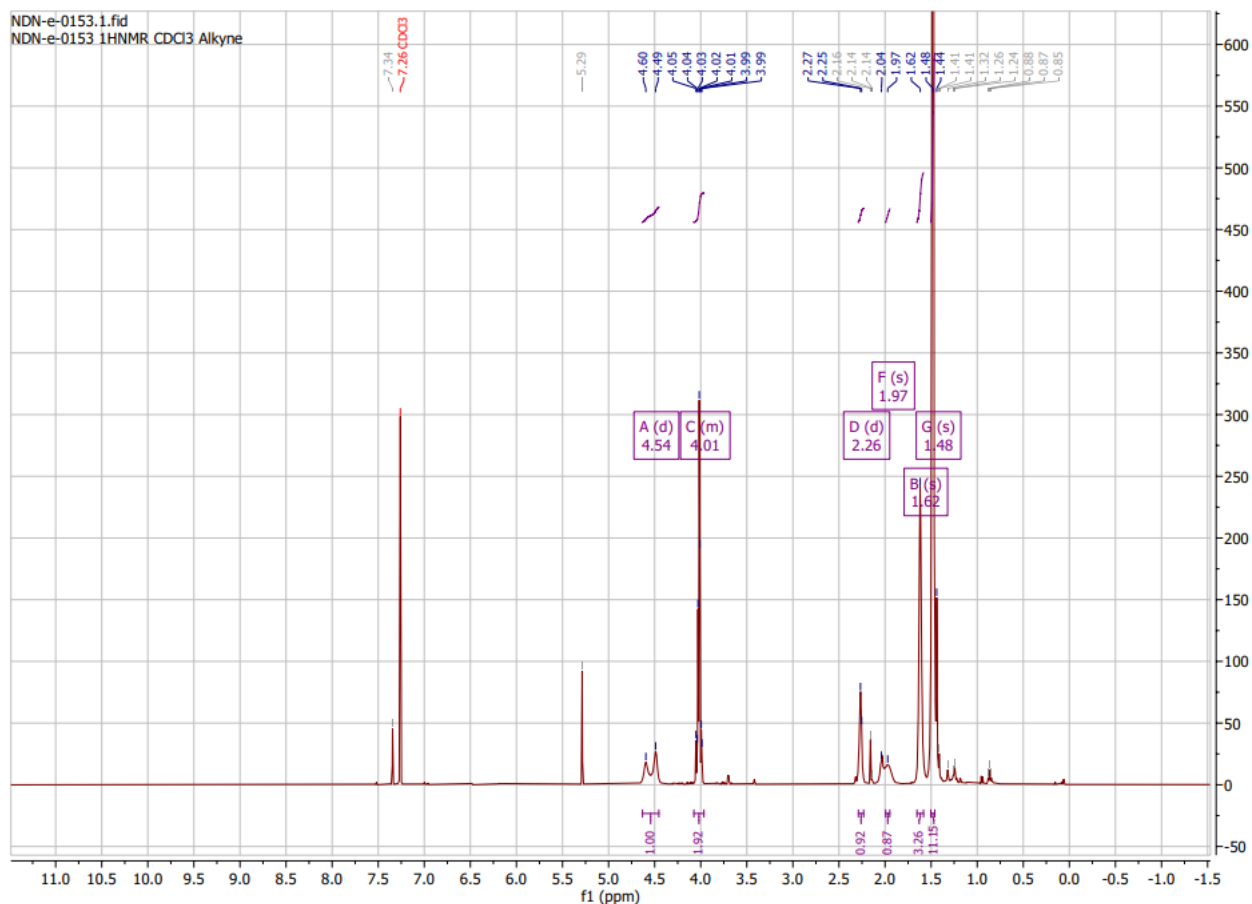


tert-butyl (R)-4-(2,2-dibromovinyl)-2,2-dimethyloxazolidine-3-carboxylate: To an 250mL oven dried flask and stir bar under argon was added Carbon tetrabromide (2.00eq, 5.79g, 17.4mmol) and dichloromethane (80mL) and the solution was cooled to  $-30^\circ\text{C}$ . A solution of triphenylphosphine (4.00eq, 9.15g, 34.9mmol) in dichloromethane (50mL) was added dropwise and the reaction was let stir 20 minutes after addition. At this point the mixture was cooled to  $-78^\circ\text{C}$  and tert-butyl (S)-4-formyl-2,2-dimethyloxazolidine-3-carboxylate (1.00eq, 2.00g, 8.72mmol) solution in dichloromethane (30mL) and triethylamine (1.00eq, 1.22mL, 8.72mmol) was added dropwise with the noticed color change to orange and the resultant solution stirred for another 10 minutes before warming to  $0^\circ\text{C}$  and stirring for 1.5 hours with a noticed color change to dark red. TLC showed conversion and reaction was quenched with sat. aq.  $\text{NaHCO}_3$  solution at which point it was moved to a separatory funnel and extracted with ether in 3 80mL portions. Extracts were dried over  $\text{Na}_2\text{SO}_4$  and concentrated in vacuo. Residue was purified via column chromatography to afford tert-butyl (R)-4-(2,2-dibromovinyl)-2,2-dimethyloxazolidine-3-carboxylate (2.94g, 87.5%) verified by  $^1\text{H}$ NMR.  $^1\text{H}$  NMR (400 MHz,  $\text{CDCl}_3$ )  $\delta$  6.45 (s, 1H), 4.51 (s, 1H), 4.10 (dd,  $J = 9.1, 6.3$  Hz, 1H), 3.79 (s, 1H), 2.17 (s, 1H), 1.59 (d,  $J = 9.8$  Hz, 3H), 1.54 – 1.40 (m, 13H).<sup>68</sup>

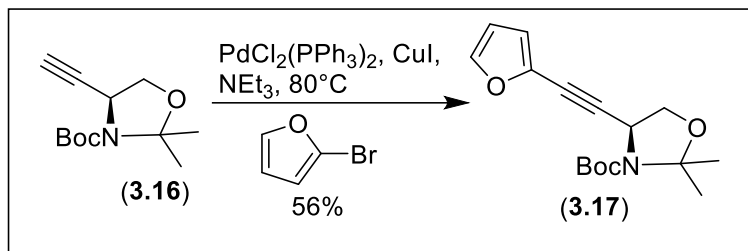




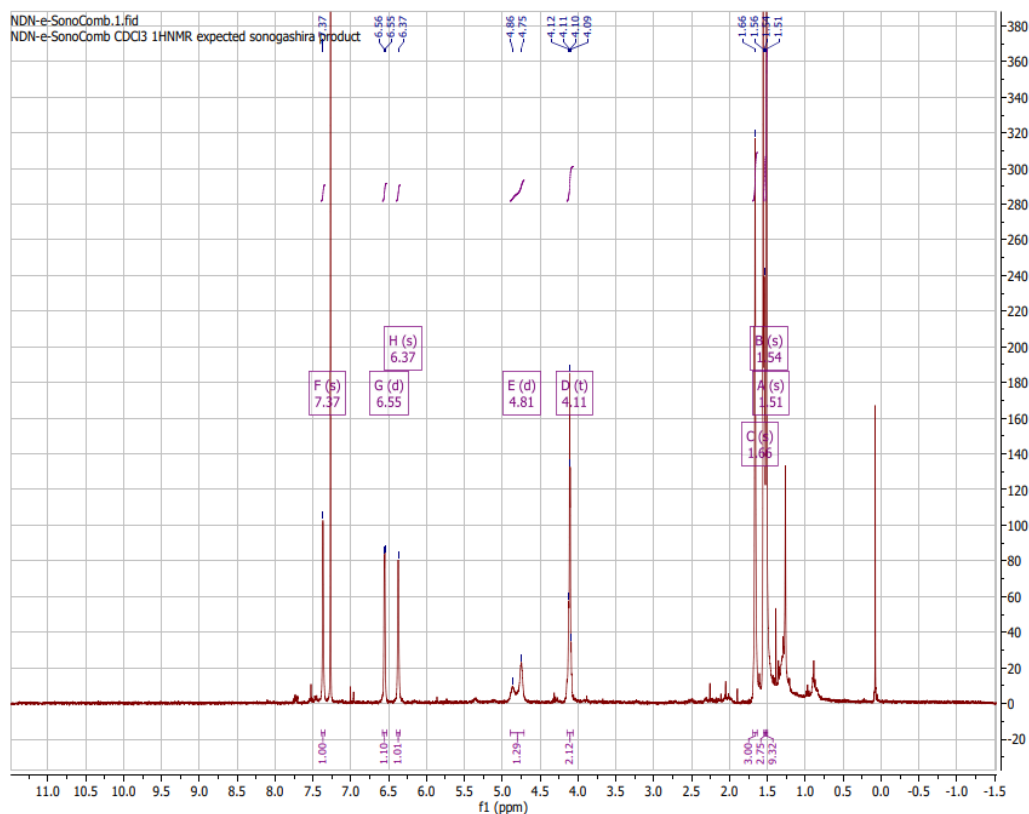
tert-butyl (R)-4-ethynyl-2,2-dimethyloxazolidine-3-carboxylate: To an 500mL oven dried flask and stir bar under argon was added tert-butyl (R)-4-(2,2-dibromovinyl)-2,2-dimethyloxazolidine-3-carboxylate (1.00eq, 9.50g, 24.7mmol) and tetrahydrofuran (150mL). This mixture was cooled to 0°C and 3M ethyl Grignard (2.00eq, 16.4mL, 49.3mmol) was added dropwise and the reaction stirred for 2 hours after which TLC showed conversion so reaction was quenched with sat. aq. NaHCO<sub>3</sub> solution and moved to a separatory funnel where it was extracted with EtOAc in 3 portions of 100mL. Extracts were dried over Na<sub>2</sub>SO<sub>4</sub> and concentrated in vacuo. The resultant residue was purified via column chromatography to yield tert-butyl (R)-4-ethynyl-2,2-dimethyloxazolidine-3-carboxylate (4.94g, 89%) verified via <sup>1</sup>H NMR. <sup>1</sup>H NMR (400 MHz, CDCl<sub>3</sub>) δ 4.54 (d, J = 42.5 Hz, 1H), 4.07 – 3.97 (m, 2H), 2.26 (d, J = 4.8 Hz, 1H), 1.97 (s, 1H), 1.62 (s, 3H), 1.48 (s, 11H).<sup>68</sup>







tert-butyl (S)-4-(furan-2-ylethynyl)-2,2-dimethyloxazolidine-3-carboxylate: To an oven dried flask and stir bar under argon and wrapped with tinfoil was added bis(triphenylphosphine) palladium (II) dichloride (PdCl<sub>2</sub>(PPh<sub>3</sub>)<sub>2</sub> (10 mol%, 0.31g, 0.43mmol), tert-butyl (S)-4-ethynyl-2,2-dimethyloxazolidine-3-carboxylate (1.00eq, 0.98g, 4.3mmol), triethylamine (10eq, 6.1mL), and 2-bromofuran (5.00eq, 3.2g, 22mmol). Solution was stirred for 15 minutes at 23°C then warmed to 40°C and stirred for 15 minutes. CuI (1 mol%, 8.3mg, 0.043mmol) was added and temperature was slowly raised to 80°C over a 30-minute period. Solution was stirred 12 hours and TLC showed full consumption of starting material alkyne. Reaction was cooled to 23°C and diluted with EtOAc. Solution was quenched with 1M HCl and transferred to a separatory funnel. Mixture was extracted with three portions of EtOAc and dried over Na<sub>2</sub>SO<sub>4</sub> and concentrated under reduced pressure. The crude product was purified via column chromatography to yield tert-butyl (S)-4-(furan-2-ylethynyl)-2,2-dimethyloxazolidine-3-carboxylate (718mg, 57% yield), a yellow-white crystalline solid. <sup>1</sup>HNMR (400MHz, CDCl<sub>3</sub>) δ ppm: 7.37 (s, 1 H), 6.55 (s, 1 H), 6.37 (s, 1 H), 4.81 (d, 1 H, J = 45.10Hz), 4.11 (t, 2 H J = 4.20Hz), 1.66 (s, 3 H), 1.54 (s, 3 H), 1.51 (s, 9 H)





## References:

1. Van Valen, L.; A New Evolutionary Law, *Evol. Theory*, **1973** 1, 1–30
2. Bentley, R.; Bennett, J. W., What Is an Antibiotic? Revisited. *Adv. Appl. Microbiol.* **2003**, 52, 303-331.
3. Silver, L. L., Challenges of antibacterial discovery. *Clin. Microbiol. Rev.* **2011**, 24 (1), 71-109.
4. Winau, F.; Westphal, O.; Winau, R., Paul Ehrlich—in search of the magic bullet. *Microbes Infect.* **2004**, 6 (8), 786-9.
5. Wright, G. D., The antibiotic resistome: the nexus of chemical and genetic diversity. *Nat. Rev. Microbiol.* **2007**, 5 (3), 175-86.
6. Wainwright, M.; Kristiansen, J. E., On the 75th anniversary of Prontosil. *Dyes Pigments* **2011**, 88 (3), 231-234.
7. Bentley, R., Different roads to discovery; Prontosil (hence sulfa drugs) and penicillin (hence beta-lactams). *J. Ind. Microbiol. Biotechnol.* **2009**, 36 (6), 775-86. 65
8. Zaman, S. B.; Hussain, M. A.; Nye, R.; Mehta, V.; Mamun, K. T.; Hossain, N., A Review on Antibiotic Resistance: Alarm Bells are Ringing. *Cureus* **2017**, 9 (6), e1403.
9. Brown, E. D.; Wright, G. D., Antibacterial drug discovery in the resistance era. *Nature* **2016**, 529 (7586), 336-43.
10. Wright, G. D., Q&A- Antibiotic resistance—where does it come from and what can we do about it? *BMC Biology* **2010**, 8.
11. Clatworthy, A. E.; Pierson, E.; Hung, D. T., Targeting virulence: a new paradigm for antimicrobial therapy. *Nat. Chem. Biol.* **2007**, 3 (9), 541-8.
12. Global Priority List of Antibiotic-Resistant Bacteria to Guide Research, Discover, and Development of New Antibiotics. *World Health Organization*, **2017**.
13. Walsh, C., Molecular mechanisms that confer antibacterial drug resistance. *Nature* **2000**, 406 (6797), 775-781.
14. Munita, J. M.; Arias, C. A., Mechanisms of Antibiotic Resistance. *Microbiol. Spectr.* **2016**, 4 (2)
15. Silhavy, T. J.; Kahne, D.; Walker, S., The bacterial cell envelope. *Cold Spring Harb. Perspect. Biol.* **2010**, 2 (5), 1-16.
16. Delcour, A. H., Outer membrane permeability and antibiotic resistance. *Biochim. Biophys. Acta.* **2009**, 1794 (5), 808-16.
17. Galdiero, S.; Falanga, A.; Cantisani, M.; Tarallo, R.; Della Pepa, M. E.; D'Orlando, V.; Galdiero, M., Microbe-host interactions: structure and role of Gram-negative bacterial porins. *Curr. Protein Pept. Sci.* **2012**, 13 (8), 843-54.
18. Sun, J.; Deng, Z.; Yan, A., Bacterial multidrug efflux pumps: mechanisms, physiology and

- pharmacological exploitations. *Biochem. Biophys. Res. Commun.* **2014**, 453 (2), 254-67.
19. Borges-Walmsley, M. I.; McKeegan, K. S.; Walmsley, A. R., Structure and function of efflux pumps that confer resistance to drugs. *Biochem. J.* **2003**, 376, 313-338.
20. Soto, S. M., Role of efflux pumps in the antibiotic resistance of bacteria embedded in a biofilm. *Virulence* **2013**, 4 (3), 223-9.
21. Martinez, J. L.; Sánchez, M. B.; Martínez-Solano, L.; Hernandez, A.; Garmendia, L.; Fajardo, A.; Alvarez-Ortega, C., Functional role of bacterial multidrug efflux pumps in microbial natural ecosystems. *FEMS Microbiol. Rev.* **2009**, 33 (2), 430-449.
22. Bush, K.; Bradford, P. A., Beta-Lactams and Beta-Lactamase Inhibitors: An Overview. *Cold Spring Harb. Perspect. Med.* **2016**, 6 (8), 1-16.
23. Magnet, S.; Blanchard, J. S., Molecular insights into aminoglycoside action and resistance. *Chem. Rev.* **2005**, 105 (2), 477-497.
24. Garneau-Tsodikova, S.; Labby, K. J., Mechanisms of Resistance to Aminoglycoside Antibiotics: Overview and Perspectives. *Medchemcomm* **2016**, 7 (1), 11-27.
25. Becker, B.; Cooper, M. A., Aminoglycoside antibiotics in the 21st century. *ACS Chem. Biol.* **2013**, 8 (1), 105-15.
26. Aldred, K. J.; Kerns, R. J.; Osheroff, N., Mechanism of quinolone action and resistance. *Biochemistry* **2014**, 53 (10), 1565-74.
27. Craft, K. M.; Townsend, S. D., The Human Milk Glycome as a Defense Against Infectious Diseases: Rationale, Challenges, and Opportunities. *ACS Infect. Dis.* **2017**, 4 (2), 77-83.
28. Schatz, A., Bugie, E., and Waksman, S. A. Streptomycin, a substance exhibiting antibiotic activity against gram-positive and gram-negative bacteria. *Proc. Soc. Exp. Biol. Med.* **1944**, 55, 66-69.
29. Becker, B.; Cooper, A. M., Aminoglycoside Antibiotics in the 21<sup>st</sup> Century. *ACS Chem. Biol.* **2013**, 8, 105-115.
30. Zhanel, G. G.; Lawson, C. D.; Zelenitsky, S.; Findlay, B.; Schweizer, F.; Adam, H.; Walkty, A.; Rubinstein, E.; Gin, A. S.; Hoban, D. J.; Lynch, J. P.; Karlowsky, J. A., Comparison of the next-generation aminoglycoside plazomicin to gentamicin, tobramycin and amikacin, *Expert Rev Anti Infect Ther.* **2012**, 10, 459-473.
31. Bottger, C. E.; Crich, D., Aminoglycosides: Time for the Resurrection of a Neglected Class of Antibacterials?, *ACS Infect. Dis.* **2020**, 6, 168-172
32. Vanhoof, R.; Sonck, P.; Hannecart-Pokorni, E., The role of lipopolysaccharide anionic binding sites in aminoglycoside uptake in *Stenotrophomonas (Xanthomonas) maltophilia*. *J. Antimicrob. Chemother.* **1995**, 35, 167-171.
33. Taber, H. W.; Mueller, J. P.; Miller, P. F.; Arrow, A. S., Bacterial uptake of aminoglycoside antibiotics.

*Microbiol Rev.* **1987**, 51, 439-457.

34. Bryan, L. E.; Van Den Elzen, H. M., Effects of Membrane-Energy Mutations and Cations on Streptomycin and Gentamicin Accumulation by Bacteria: a Model for Entry of Streptomycin and Gentamicin in Susceptible and Resistant Bacteria. *Antimicrob. Agents Chemother.* **1977**, 12, 163-177.
35. Davis, B. D.; Chen, L. L.; Tai, P. C., Misread protein creates membrane channels: an essential step in the bactericidal action of aminoglycosides. *Proc Natl Acad Sci.* **1986**, 83, 6164-6168
36. Davies, J.; Gorini, L.; Davis, B. D., Misreading of RNA codewords induced by aminoglycoside antibiotics. *Mol. Pharmacol.* **1965**, 1, 93-106.
37. Matt, T.; Ng, C. L.; Lang, K.; Sha, S.-H.; Akbergenov, R.; Shcherbakov, D.; Meyer, M.; Duscha, S.; Xie, J.; Dubbaka, S. R.; Perez-Fernandez, D.; Vasella, A.; Ramakrishnan, V.; Schacht, J.; Böttger, E. C., Dissociation of antibacterial activity and aminoglycoside ototoxicity in the 4-monosubstituted 2-deoxystreptamine apramycin. *Proc Natl Acad Sci.* **2012**, 109, 10984-10989.
38. Houghton, J. L.; Green, K. D.; Chen, W.; Garneau-Tsodikova, S., The future of aminoglycosides: the end or renaissance?. *ChemBioChem.* **2010**, 11, 880-902.
39. Perez-Fernandez, D.; Shcherbakov, D.; Matt, T.; Leong, N. C.; Kudyba, I.; Duscha, S.; Boukari, H.; Patak, R.; Dubbaka, S. R.; Lang, K.; Meyer, M.; Akbergenov, R.; Freihofer, P.; Vaddi, S.; Thommes, P.; Ramakrishnan, V.; Vasella, A.; Böttger, E. C., In Vivo Efficacy of Apramycin in Murine Infection Models. *Nat Commun.* **2014**, 5.
40. Macfarlane, E. L. A., Kwasnicka, A., and Hancock, R. E. W. Role of *Pseudomonas aeruginosa* PhoP-PhoQ in resistance to antimicrobial cationic peptides and aminoglycosides. *Microbiology.* **2000**, 146, 2543-2554.
41. Kwon, D. H., and Lu, C. D. Polyamines induce resistance to cationic peptide, aminoglycoside, and quinolone antibiotics in *Pseudomonas aeruginosa* PAO1. *Antimicrob. Agents Chemother.* **2006**, 50, 1615-1622.
42. Wang, X. Y., and Quinn, P. J. Lipopolysaccharide: Biosynthetic pathway and structure modification. *Prog. Lipid Res.* **2010**, 49, 97-107.
43. Bryan, L. E.; Kowand, S. K.; Van Den Elzen, H. M., Mechanism of aminoglycoside antibiotic resistance in anaerobic bacteria: *Clostridium perfringens* and *Bacteroides fragilis* *Antimicrob. Agents Chemother.* **1979**, 15, 7-13.
44. Arrow, A. S., and Taber, H. W. Streptomycin accumulation by *Bacillus subtilis* requires both a membrane-potential and cytochrome aa3. *Antimicrob. Agents Chemother.* **1986**, 29, 141-146
45. McEnroe, A. S., and Taber, H. W. Correlation between cytochrome-aa3 concentrations and streptomycin accumulation in *Bacillus subtilis*. *Antimicrob. Agents Chemother.* **1984**, 26, 507-512.
46. Muir, M. E., Hanwell, D. R., and Wallace, B. J. Characterization of a respiratory mutant of *Escherichia*

- coli with reduced uptake of aminoglycoside antibiotics. *Biochim. Biophys. Acta.* **1984**, 638, 234–241.
47. Magnet, S.; Blanchard, J. S., Molecular insights into aminoglycoside action and resistance. *Chem. Rev.* **2005**, 105, 477-498.
48. Vakulenko, S. B.; Mobashery, S., Versatility of aminoglycosides and prospects for their future. *Clin. Microbiol. Rev.* **2003**, 16, 430-450.
49. Wolf, E.; Vassilev, A.; Makino, Y.; Sali, A.; Nakatani, Y.; Burley, S. K., Crystal structure of a GCN5-related N-acetyltransferase: *Serratia marcescens* aminoglycoside 3-N-acetyltransferase. *Cell.* **1998**, 94, 439-449.
50. Gray, G. S.; Fitch, W. M., Evolution of antibiotic resistance genes: the DNA sequence of a kanamycin resistance gene from *Staphylococcus aureus*. *Mol. Biol. Evol.* **1983**, 1, 57-66.
51. Fong, D. H.; Berghuis, A. M., Substrate promiscuity of an aminoglycoside antibiotic resistance enzyme via target mimicry. *EMBO J.* **2002**, 21, 2323-2331.
52. Azucena, E.; Grapsas, I.; Mobashery, S., Aminoglycoside-modifying enzymes: mechanisms of catalytic processes and inhibition *J. Am. Chem. Soc.* **1997**, 119, 2317- 2318.
53. Bacot-Davis, V. R.; Bassenden, A. V.; Berghuis, A. M., Drug-target networks in aminoglycoside resistance: hierarchy of priority in structural drug design. *MedChemComm.* **2016**, 7, 103-113.
54. Doi, Y.; Yokoyama, K.; Yamane, K.; Wachino, J.-i.; Shibata, N.; Yagi, T.; Shibayama, K.; Kato, H.; Arakawa, Y., Plasmid-Mediated 16S rRNA Methylase in *Serratia marcescens* Conferring High-Level Resistance to Aminoglycosides *Antimicrob. Agents Chemother.* **2004**, 48, 491-496.
55. Cundliffe, E., HOW ANTIBIOTIC-PRODUCING ORGANISMS AVOID SUICIDE. *Annual Reviews in Microbiology.* **1989**, 43, 207-233.
56. Wachino, J.-i., and Arakawa, Y. Exogenously acquired 16S rRNA methyltransferases found in aminoglycoside-resistant pathogenic Gram-negative bacteria: An update. *Drug Resistance Updates.* **2012**, 15, 133–148.
57. Doi, Y., Garcia, D. D., Adams, J., and Paterson, D. L. Coproduction of novel 16S rRNA methylase RmtD and metallo-beta-lactamase SPM-1 in a panresistant *Pseudomonas aeruginosa* isolate from Brazil. *Antimicrob. Agents Chemother.* **2007**, 51, 852–856.
58. Yokoyama, K., Doi, Y., Yamane, K., Kurokawa, H., Shibata, N., Shibayama, K., Yagi, T., Kato, H., and Arakawa, Y. Acquisition of 16S rRNA methylase gene in *Pseudomonas aeruginosa*. *Lancet.* **2003**, 362, 1888–1893.
59. Galimand, M., Courvalin, P., and Lambert, T. Plasmid-mediated high-level resistance to aminoglycosides in Enterobacteriaceae due to 16S rRNA methylation. *Antimicrob. Agents Chemother.* **2003**, 47, 2565–2571.
60. Gonzalez-Zorn, B., Teshager, T., Casas, M., Porrero, M. C., Moreno, M. A., Courvalin, P., and Dominguez, L. armA and aminoglycoside resistance in *Escherichia coli*. *Emerging Infect. Dis.* **2005**, 11,

954–956.

61. Wachino, J. I., Shibayama, K., Kurokawa, H., Kimura, K., Yamane, K., Suzuki, S., Shibata, N., Ike, Y., and Arakawa, Y. Novel plasmid-mediated 16S rRNA m(1)A1408 methyltransferase, NpmA, found in a clinically isolated *Escherichia coli* strain resistant to structurally diverse aminoglycosides. *Antimicrob. Agents Chemother.* **2007**, 51, 4401–4409.
62. Wachino, J. I., Yamane, K., Shibayama, K., Kurokawa, H., Shibata, N., Suzuki, S., Doi, Y., Kimura, K., Ike, Y., and Arakawa, Y. Novel plasmid-mediated 16S rRNA methylase, RmtC, found in a *Proteus mirabilis* isolate demonstrating extraordinary high-level resistance against various aminoglycosides. *Antimicrob. Agents Chemother.* **2006**, 50, 178–184.
63. Karthikeyan, K., Thirunarayan, M. A., and Krishnan, P. Coexistence of bla(OXA-23) with bla(NDM-1) and armA in clinical isolates of *Acinetobacter baumannii* from India. *J. Antimicrob. Chemother.* **2010**, 65, 2253–2254.
64. Hotta, K.; Sunada, A.; Ikeda, Y.; Kondo, S., Double Stage Activity in Aminoglycoside Antibiotics. *The Journal of antibiotics.* **2000**, 53, 1168-1174.
65. Mata, G.; Leudtke, W. N., Stereoselective N-Glycosylation of 2-Deoxythioribosides for Fluorescent Nucleoside Synthesis. *Journal of Organic Chemistry*, **2012**, 77, 20, 9006–9017.
66. Noyori, R.; Suga, S.; Kawai, K.; Okada, S.; Kitamura, M.; Oguni, N.; Hayashi, M.; Kaneko, T.; Matsuda, Y., Enantioselective addition of diorganozincs to aldehydes catalyzed by  $\beta$ -amino alcohols. *Journal of Organometallic Chemistry*, **1990**, 382 19-37.
67. Dondoni, A.; Perrone, D, SYNTHESIS OF 1,1-DIMETHYLETHYL (S)-4-FORMYL-2,2-DIMETHYL-3-OXAZOLIDINECARBOXYLATE BY OXIDATION OF THE ALCOHOL. *Org. Synth.* **2000**, 77, 64.
68. Yamakawa, T.; Ideue, E.; Iwaki, Y.; Sato, A.; Tokuyama, H.; Shimokawa, J.; Fukuyama, T., Total synthesis of tryprostatins A and B. *Tetrahedron*, **2011**, 67, 35, 6547-6560.
69. Liu, F. Myers, A. IPN: WO 2019/0790706 A1, 25, April, 2019.
70. Myers, A. Seiple, I. Zhang, Z. IPN: WO 2014/165792 A2, 9 October, 2014.
71. Schlessinger, R.; Pettus, R. R. T.; Springer, P. J.; Hoogsteen, K., Diastereoselective Diels-Alder Reactions Using Furan Substituted with a Nonracemic Amine. *J. Org. Chem.* **1994**, 59, 3246-3247.
72. Schlessinger, H. R; Bergstrom, P. C., Diastereoselective Diels-Alder reactions of nonracemic 3- and 4-amino furans bound to polystyrene. A comparison of these reactions to their solution state analogues. *Tetrahedron Letters*, **1996**, 37, 13, 2133-2136.
73. Enders, D.; Kipphardt, H.; Gerdes, P.; Brena-Valle, J. L.; Bhuhsan, V., Large scale preparation of versatile chiral auxiliaries derived from (S)-proline. *Bull Soc. Chim. Belg.* **1988**, 97, 8-9.
74. Wright, M. P.; Seiple, B. I.; Myers, G. A., The Evolving Role of Chemical Synthesis in Antibacterial

Drug Discovery. *Angewandte Chemie*, **2014**, 53, 1-7.

75. Crich, D.; Smith, M., 1-Benzenesulfinyl piperidine/trifluoromethanesulfonic anhydride: a potent combination of shelf-stable reagents for the low-temperature conversion of thioglycosides to glycosyl triflates and for the formation of diverse glycosidic linkages. *J. Am. Chem. Soc.* **2001**, 123, 9015-9020.

76. Gao, M.; Chen, Y.; Tan, S; Reibenspies, H. J.; Zingaro, A. R., Syntheses of 1-thio-D-xylose and D-ribose esters of diorganoarsinous acids and their anticancer activity. *Heteroatom Chemistry*. **2008**, 19, 199-206.

77. Harwood, J. S.; Palkowitz, D. M.; Gannett, N. C.; Perez, P.; Yao, Z.; Sun, L.; Abruna, D. H.; Anderson, L. A.; Baran, S. P., Modular terpene synthesis enabled by mild electrochemical couplings. *Science*. **2022**, 375, 6582, 745-752.